The ZmASR1 protein influences branched-chain amino acid biosynthesis and maintains kernel yield in maize under water-limited conditions

Laëtitia Virlouvet, Marie Pierre Jacquemot, Denise Gerentes, Helene Corti, Sophie Bouton, Françoise Gilard, Benoit B. Valot, Jacques Trouverie, Guillaume Tcherkez, Matthieu M. Falque, et al.

The ZmASR1 Protein Influences Branched-Chain Amino Acid Biosynthesis and Maintains Kernel Yield in Maize under Water-Limited Conditions[1][W][OA]

Laetitia Virlouvet, Marie-Pierre Jacquemot, Denise Gerentes, Hélène Corti, Sophie Bouton[2], Françoise Gilard, Benoît Valot, Jacques Trouverie[3], Guillaume Tcherkez, Matthieu Falque, Catherine Damerval, Peter Rogowsky, Pascual Perez[4], Graham Noctor, Michel Zivy, and Sylvie Coursol*

Université Paris-Sud, UMR 320/UMR 8120 Génétique Végétale, F–91190 Gif-sur-Yvette, France (L.V.); INRA, UMR 320/UMR 8120 Génétique Végétale, F–91190 Gif-sur-Yvette, France (M.-P.J., H.C., S.B., B.V., J.T., M.F., S.C.); Biogemma Auvergne, F–63028 Clermont-Ferrand cedex, France (D.G., P.P.); CNRS, UMR 8618 Institut de Biotechnologie des Plantes, F–91405 Orsay, France (F.G.); Université Paris-Sud, UMR 8618 Institut de Biotechnologie des Plantes, F–91405 Orsay, France (G.T., G.N.); CNRS, UMR 320/UMR 8120 Génétique Végétale, F–91190 Gif-sur-Yvette, France (C.D., M.Z.); and INRA, UMR 879 Reproduction et Développement des Plantes, F–69364 Lyon, France (P.R.)

Abscisic acid-, stress-, and ripening-induced (ASR) proteins were first described about 15 years ago as accumulating to high levels during plant developmental processes and in response to diverse stresses. Currently, the effects of ASRs on water deficit tolerance and the ways in which their physiological and biochemical functions lead to this stress tolerance remain poorly understood. Here, we characterized the *ASR* gene family from maize (*Zea mays*), which contains nine paralogous genes, and showed that maize ASR1 (ZmASR1) was encoded by one of the most highly expressed paralogs. Ectopic expression of *ZmASR1* had a large overall impact on maize yield that was maintained under water-limited stress conditions in the field. Comparative transcriptomic and proteomic analyses of wild-type and *ZmASR1*-overexpressing leaves led to the identification of three transcripts and 16 proteins up- or down-regulated by ZmASR1. The majority of them were involved in primary and/or cellular metabolic processes, including branched-chain amino acid (BCAA) biosynthesis. Metabolomic and transcript analyses further indicated that *ZmASR1*-overexpressing plants showed a decrease in BCAA compounds and changes in BCAA-related gene expression in comparison with wild-type plants. Interestingly, within-group correlation matrix analysis revealed a close link between 13 decreased metabolites in *ZmASR1*-overexpressing leaves, including two BCAAs. Among these 13 metabolites, six were previously shown to be negatively correlated to biomass, suggesting that ZmASR1-dependent regulation of these 13 metabolites might contribute to regulate leaf growth, resulting in improvement in kernel yield.

Since one-third of the world's food is produced on irrigated land (Food and Agriculture Organization of the United Nations, 2008), the likely impacts of recurrent heat waves and water stress episodes on global food production are numerous. In the European heat wave of 2003, crop production was reduced by around 30% (Ciais et al., 2005). In maize (*Zea mays*), the most significant reductions in end-of-season kernel yields are observed when water deficit occurs during the flowering stage, either just before floral initiation or immediately after pollination, because of the impact of water deficit on ovary and young kernel abortions (Claassen, 1970; Boyer and Westgate, 2004). Water deficit during the vegetative growth phase also leads to reductions in overall productivity through reductions in kernel numbers (Boyer and Westgate, 2004). Finally, late-stage water deficit during the kernel-filling period can lead to reductions in yield, depending upon the dry matter reserves in the plant (McPherson and Boyer, 1977).

Trait-based approaches considering maize drought avoidance and dehydration tolerance mechanisms have been relatively slow to progress, as judged by the adoption of improved varieties (Salekdeh et al., 2009). Transgenic maize plants expressing the *betA*

[1] This work was supported by the Génoplante projects B06 and WaterLess (grant no. ANR05–GPLA–034–05) and by a Ph.D. research fellowship of the Université Paris-Sud 11 to L.V.

[2] Present address: Université Picardie Jules Verne, EA3900 Biologie des Plantes et Contrôle des Insectes Ravageurs, F–80039 Amiens, France.

[3] Present address: INRA, UMR 950 Ecophysiologie Végétale, Agronomie et Nutritions N, C, S, F–14032 Caen, France.

[4] Present address: Field Crop Division, Limagrain Europe, Site de la Garenne, F–63720 Chappes, France.

* Corresponding author; e-mail coursol@moulon.inra.fr.

The author responsible for distribution of materials integral to the findings presented in this article in accordance with the policy described in the Instructions for Authors (www.plantphysiol.org) is: Sylvie Coursol (coursol@moulon.inra.fr).

[W] The online version of this article contains Web-only data.

[OA] Open Access articles can be viewed online without a subscription.

www.plantphysiol.org/cgi/doi/10.1104/pp.111.176818

gene from *Escherichia coli* encoding choline dehydrogenase, a key enzyme in the biosynthesis of Gly betaine from choline, showed enhanced Gly betaine accumulation, resulting in greater kernel yield after drought stress in field tests (Quan et al., 2004). Expression of a maize CAAT box transcription factor, *Z. mays* nuclear factor Y B subunit 2 (ZmNF-YB2), has also been shown to confer drought tolerance and enhanced photosynthetic capacity under drought stress, with improvements in kernel yield in maize (Nelson et al., 2007). Additionally, two members of a family of bacterial RNA chaperones, cold shock protein A (CspA) from *E. coli* and CspB from *Bacillus subtilis*, were shown to confer vegetative tolerance and improved end-of-season kernel yield under water-limiting conditions in maize (Castiglioni et al., 2008). These studies clearly demonstrate that maize plants are amenable to improved water deficit tolerance through multiple mechanisms of action.

Having specific target traits and genes can markedly accelerate progress through the marker-assisted selection of parents and progeny in early generations (Tuberosa and Salvi, 2006). We used a proteomics strategy, with the use of a recombinant inbred line population derived from the cross between the maize inbred lines MBS847 and F2, differing in yield under water deprivation conditions, to identify candidate proteins associated with water stress response in maize (de Vienne et al., 1999). The protein quantity profiling of all individuals in the segregating population made it possible to treat the quantity of each protein as a quantitative trait and to identify a quantitative trait locus (QTL) for protein quantity, hereafter named protein quantity locus (PQL) according to Damerval et al. (1994). When the PQL colocated with a QTL related to water deficit response, a causal relationship could be inferred between the protein level and the trait variation. Furthermore, when the gene encoding the protein also colocated, it could be seen as a candidate gene. Among the identified candidate genes was a member of the abscisic acid-, stress-, and ripening-induced (*ASR*) gene family, *ZmASR1*, which colocated with its PQL and QTLs for leaf senescence and anthesis-silking interval (de Vienne et al., 1999; Jeanneau et al., 2002). These associations were validated by the observation that transgenic maize lines misexpressing *ZmASR1* showed significant changes in leaf senescence under mild water deficit conditions in the field (Jeanneau et al., 2002). Interestingly, transgenic Arabidopsis (*Arabidopsis thaliana*) plants overexpressing an *ASR* gene from *Lilium longiflorum* (*LLA23*) or banana (*Musa paradisiaca*; *MpASR*) exhibited enhanced capacity to survive in water-limited conditions (Yang et al., 2005; Liu et al., 2010). Overexpression of the tomato (*Solanum lycopersicum*) *ASR1* gene (*SlASR1*) in tobacco (*Nicotiana tabacum*) plants also resulted in decreased rates of water loss (Kalifa et al., 2004b). Together, these results suggest that water deficit tolerance is mediated at least in part through ASR proteins.

The ASR proteins are highly charged, hydrophilic, and low-M_r proteins that are widely present in the plant kingdom, except in the Brassicaceae family (for review, see Carrari et al., 2004; Battaglia et al., 2008). Since their discovery more than a decade ago, they have been described as accumulating to high levels during plant developmental processes, such as fruit ripening, pollen maturation, and Glc metabolism (Iusem et al., 1993; Wang et al., 1998; Cakir et al., 2003; Frankel et al., 2007; Yang et al., 2008), and in response to diverse stresses, including water deficit, salt, cold, limited light, and, lately, pathogen attack (Schneider et al., 1997; Riccardi et al., 1998; Vaidyanathan et al., 1999; Huang et al., 2000; Maskin et al., 2001; Kalifa et al., 2004b; Liu et al., 2010; Philippe et al., 2010; Henry et al., 2011). Nevertheless, it is noteworthy that their exact function remains enigmatic. Indeed, the molecular mechanisms underlying the biological roles of the ASR proteins cannot be deduced simply by sequence homology with other known proteins. SlASR1 and the grape (*Vitis vinifera*) ASR protein, VvMSA (for maturation-, stress-, and abscisic acid-induced protein), have been shown to possess DNA-binding activity (Cakir et al., 2003; Kalifa et al., 2004a; Rom et al., 2006; Maskin et al., 2007; Shkolnik and Bar-Zvi, 2008). On the basis of such findings, these ASR proteins have been proposed to regulate the transcription of sugar- and abiotic stress-regulated genes in fruit and vegetative tissues, respectively (Cakir et al., 2003; Kalifa et al., 2004b; Frankel et al., 2007; Saumonneau et al., 2008). However, a dual function of LLA23 and SlASR1 proteins as a regulator and a protective molecule upon water deficit has also been proposed (Yang et al., 2005, 2008; Konrad and Bar-Zvi, 2008).

To validate further the candidate gene *ZmASR1* and gain insight into its function, we characterized the *ASR* gene family of maize. We showed that *ZmASR1* was one of the most highly expressed *ASR* genes in maize and found evidence that its expression had a large overall impact on maize vegetative productivity and yield that was maintained under water-limited stress conditions in the field. We identified 25 genes that were either transcriptionally or posttranscriptionally regulated by ZmASR1, of which seven were involved in branched-chain amino acid (BCAA) biosynthesis. Our studies further revealed a close link between 13 decreased metabolites in *ZmASR1*-overexpressing leaves, including two BCAAs, and support the idea that ZmASR1-dependent regulation of BCAA biosynthetic genes might contribute to yield improvement.

RESULTS

ZmASR1 Belongs to the Maize *ASR* Gene Family, Which Consists of at Least Nine Members

To identify *ZmASR* genes, we first analyzed the public databases for the presence of putative *ASR* coding sequences in maize using the ZmASR1 protein

sequence as the query (Riccardi et al., 1998). The search was then extended to maize genomic contigs (The Institute for Genomic Research), high-throughput genomic sequences, and the recently released maize genomic sequence (Schnable et al., 2009), which were matched with the EST sequences and used to design specific primers for DNA and cDNA amplification in maize lines used for mapping analysis and transgenesis. This led to the identification of nine *ZmASR* genes in the maize genome (Fig. 1; Supplemental Tables S1 and S2), including the published gene *Bss1* (for bundle sheath strands-specific gene 1; Furumoto et al., 2000), renamed hereafter *ZmASR4*. *ZmASR1* to *ZmASR7-3* mapped to five of the 10 maize chromosomes, with chromosomes 2 and 10 harboring two loci each and chromosome 3 harboring three loci (Supplemental Table S1). *ZmASR7-1* and *ZmASR7-2* were separated by 3 kb, whereas *ZmASR7-3* was separated from this cluster by approximately 100 kb. When the nucleotide sequences of the nine *ZmASR* cDNAs were aligned, sequence identity values of 15% to 97% were observed between the individual maize genes (Supplemental Table S3). All *ZmASR* genes possessed a conserved structure composed of two exons and one intron,

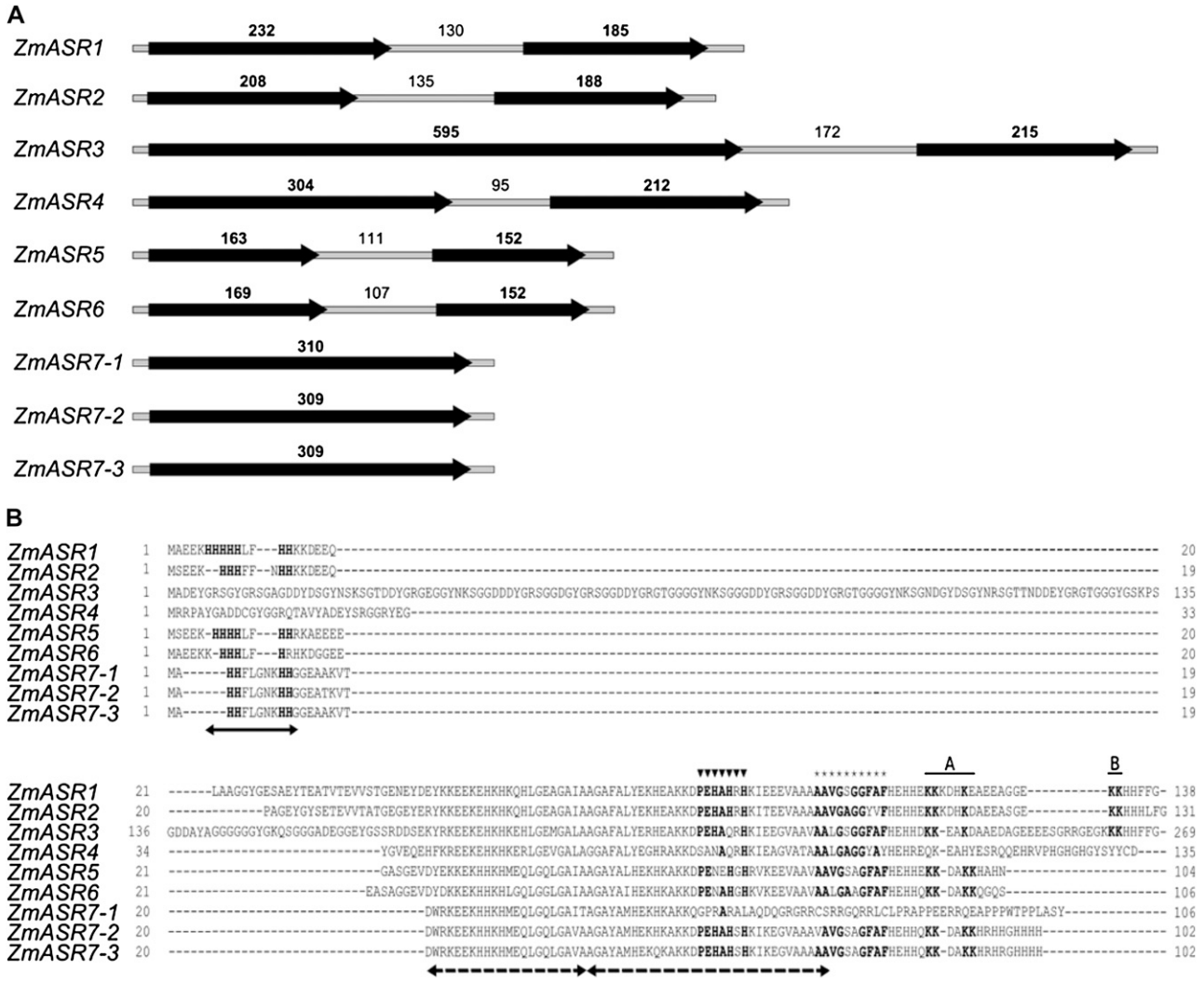

Figure 1. Gene structure of *ZmASR* genes. A, Schematic drawing of the exon/intron structure of *ZmASR* genes. Black arrows and thin gray bars indicate exons (boldface numbers) and introns (lightface numbers), respectively, the sizes of which are in bp. B, Alignment of the deduced amino acid sequences of *ZmASR* genes. Arrows denote the two highly conserved regions of ASR proteins: a small N-terminal consensus of approximately 18 to 20 amino acids containing a stretch of six His residues (solid arrow) and a large C-terminal region containing two ABA/WDS signatures (dashed arrows). Amino acid positions determined to be the Zn^{2+}-dependent DNA-binding activity domain and a sequence possibly hindering DNA binding of the SlASR1 protein (Rom et al., 2006) are marked with triangles and stars, respectively. Amino acid positions determined to be the A and B regions of the bipartite nuclear localization signal of the LLA23 protein (Wang et al., 2005) are overlined. Amino acids identical to LLA23 or SlASR1 proteins are shown in boldface.

except *ZmASR7-1*, *ZmASR7-2*, and *ZmASR7-3*, whose first and second exons were fused (Fig. 1A). This fusion between exon 1 and exon 2 was also found in sorghum (*Sorghum bicolor*) *SbASR6* and *SbASR7*, suggesting that it took place before the divergence of those two species (Supplemental Table S4). In general, the length of exons 1 and 2 was conserved (approximately 200 bp), with the exception of exon 1 of *ZmASR3*, which was three times longer, like its barley (*Hordeum vulgare*), sorghum, and rice (*Oryza sativa*) counterparts (Supplemental Table S4).

The maize *ASR* loci encoded small proteins of 102 to 269 amino acid long that met the hydrophilin criteria (Garay-Arroyo et al., 2000), in that their GRAVY index was between −1.13 and −1.37 and 8% to 28% of their amino acid residues are Gly, and were predicted to be "natively unfolded" in solution, given their enrichment in disorder-promoting charged amino acids (Supplemental Table S4; Goldgur et al., 2007). They all contained the two ASR-specific conserved motifs (e.g. a small N-terminal consensus of 18–20 amino acids containing a typical stretch of six His residues and a large C-terminal region of at least 80 amino acids containing two abscisic acid [ABA]/water deficit stress [WDS] signatures; Canel et al., 1995; Padmanabhan et al., 1997), except ZmASR3 and ZmASR4, which did not possess the N-terminal His-rich domain (Fig. 1B; Supplemental Table S4). The first exon of *ZmASR3* encoded an additional domain that was not conserved in other ZmASR proteins. Additionally, *ZmASR7-1* presented a single nucleotide insertion in a position corresponding to amino acid 57 within the second ABA/WDS signature, leading to a frameshift and consequently to a unique and maize-specific deduced amino acid sequence at the C terminus (Fig. 1B). With the exception of ZmASR4 and ZmASR5, ZmASR proteins contained a sequence motif at the C terminus (Fig. 1B; Supplemental Table S4), presenting highest identity (71%–86%) with the Zn^{2+}-dependent DNA-binding activity domain of the SlASR1 protein (Rom et al., 2006). Close examination of the C-terminal extremity of ZmASR1, ZmASR2, and ZmASR3 revealed the presence of a region structurally similar to the bipartite nuclear localization signal of LLA23 (Fig. 1B; Supplemental Table S4; Wang et al., 2005), while five other ZmASR proteins presented only the first motif (A in Fig. 1B) but lacked the second motif (B in Fig. 1B).

To assess the diversity of the *ASR* gene family beyond maize, a phylogenetic tree was constructed that included the nine maize genes and 91 related genes from representatives of different groups of Spermatophyta found in the data banks (Supplemental Fig. S1). In the case of rice, we adopted the nomenclature published during the time course of this study (Philippe et al., 2010). Maximum likelihood and Bayesian reconstruction methods were congruent and confirmed the previously established division of plant ASR proteins into three distinct clades corresponding to conifer, eudicot, and monocot sequences (Supplemental Fig. S1; Frankel et al., 2007). By adding all available maize sequences, we showed that within monocots, the Commelinid sequences form a monophyletic group, with Poaceae sequences falling into two distinct clades, the I-1/I-2/I-3 clade and the II-1/II-2 clade (Supplemental Fig. S1). Within the I-1/I-2/I-3 clade, *ZmASR1*, *ZmASR2*, *ZmASR3*, and *ZmASR4* were related to *SbASR1*, *SbASR2*, *SbASR3*, and *OsASR6*, respectively (Supplemental Fig. S1). Within the II-1/II-2 clade, *ZmASR5* and *ZmASR6* were related to *SbASR5* and *SbASR4*, respectively, while *ZmASR7-1*, *ZmASR7-2*, and *ZmASR7-3* appeared as three recent paralogs that were related to *SbASR7* (Supplemental Fig. S1).

Response of *ZmASR* Transcript Levels to Water Deficit and Water Stress-Related Treatments

To investigate the role of the different *ZmASR* genes in the maize plant and under water stress conditions, quantitative reverse transcription (qRT)-PCR was used to monitor their transcript levels in leaf and kernel tissues at different developmental stages, the growth of both tissues being very sensitive to water deficit, and root tissue, which partly maintains growth under water deficit (Westgate and Steudle, 1985). Transcript levels of *ZmASR6*, *ZmASR7-2*, and *ZmASR7-3* were not quantified because it was not possible to design gene-specific primers of sufficient quality for qRT-PCR. The relative abundance of the other six *ZmASR* amplicons could be compared, as we showed that the PCR efficiency for each gene was very similar (see "Materials and Methods").

Under well-watered conditions, all the *ZmASR* genes tested were transcribed in leaf, kernel, and root tissues (Fig. 2). In leaves, the expression of *ZmASR1* displayed a bell-shaped expression pattern (Fig. 2A), peaking at 10 cm from the leaf insertion point (e.g. beyond the growing zone, which has a constant length of 7–8 cm in maize; Tardieu et al., 2000). The transcript levels of *ZmASR3*, *ZmASR4*, *ZmASR5*, and *ZmASR7-1* increased along the leaf, while the transcript levels of *ZmASR2* were rather stable along the segments from 2 to 10 cm and decreased in the mature part of the leaf (Fig. 2A). In unfertilized and fertilized caryopses, the transcript levels of *ZmASR1*, *ZmASR2*, and *ZmASR3* displayed a bell-shaped expression pattern, which peaked at 0, 7, and 9 d after pollination (DAP), respectively, and remained rather stable after 12 DAP (Fig. 2, F and G). The transcript levels of *ZmASR4* increased moderately during the filling stage, whereas expression of *ZmASR5* and *ZmASR7-1* peaked at 7 DAP and, after a drop at 12 DAP, remained rather stable throughout development (Fig. 2, F and G). Under water deficit conditions, statistically significant transcript level increases were observed for *ZmASR1*, *ZmASR2*, *ZmASR4*, and *ZmASR7-1* in leaves (Fig. 2A) but only for *ZmASR4* in kernels (Fig. 2G).

For plants, the responses to water deficit include both ABA-dependent and ABA-independent pathways (Nakashima et al., 2009). Moreover, ABA induces some *ASR* genes in a range of plant species, including

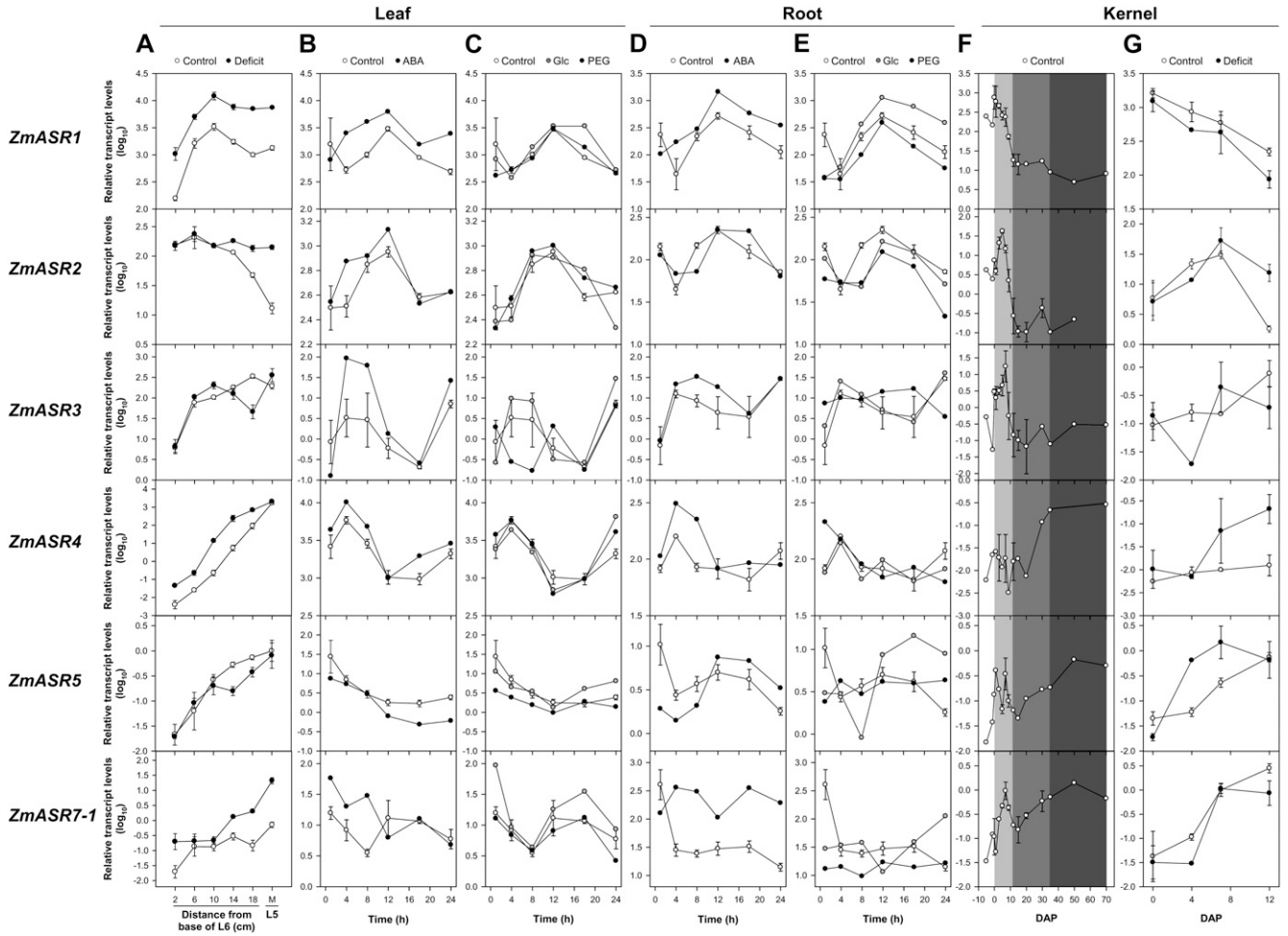

Figure 2. Transcript levels of *ZmASR* genes in leaf, root, and kernel tissues. A, *ZmASR* transcript levels in different leaf sections of B73 plants grown under well-watered (control) or water deficit (deficit) conditions. L5, Mature leaf 5; L6, growing leaf 6; M, middle of the fifth leaf blade. B to E, *ZmASR* transcript levels in leaves (B and C) and roots (D and E) from 10-d-old F2 plantlets supplied in continuous light during 24 h with culture medium (control) complemented with 3.7 μM ABA (B and D), 1% (w/v) Glc (C and E), or 7% (w/v) PEG 8000 (C and E). F and G, *ZmASR* transcript levels in developing kernels from A188 (F) or MBS847 (G) plants grown under well-watered (control) or water deficit (deficit; water interruption 7 d before pollination) conditions. The light gray, gray, and dark gray boxes indicate the early, filling, and desiccation phases of the maize kernel, respectively. qRT-PCR was performed on total RNA of the indicated tissues using gene-specific primers (Supplemental Table S2). Transcript levels were normalized against the stable endogenous *ZmGRP2* gene and shown relative to *ZmASR5* transcript levels in the middle of the fifth leaf blade in control conditions. Values represent means of three biological replicates ± SE.

tomato, tobacco, grape, banana, sugarcane (*Saccharum officinarum*), and rice (Rossi et al., 1998; Sugiharto et al., 2002; Cakir et al., 2003; Takasaki et al., 2008; Henry et al., 2011). Sugars such as Glc also exhibit interactions with ABA in controlling seedling development (Rolland et al., 2006), and grape and tomato ASR proteins may be involved in Glc metabolism (Cakir et al., 2003; Frankel et al., 2007). Additionally, polyethylene glycol (PEG)-induced water stress increases tomato, potato (*Solanum tuberosum*), and sugarcane *ASR* transcript levels (Amitai-Zeigerson et al., 1995; Huang et al., 2000; Doczi et al., 2002; Sugiharto et al., 2002). Therefore, we also studied *ZmASR* transcript levels in response to exogenous ABA (3.7 μM), Glc (1%), and PEG (7%) treatments. Transcript levels of *ZmASR1*, *ZmASR2*, *ZmASR3*, and *ZmASR4* were up-regulated between 4 and 18 h in control leaves and roots, while those of *ZmASR5* were slightly down-regulated after 4 h and up-regulated at 12 h in control leaves and roots, respectively (Fig. 2, B and D). Comparatively, transcript levels of *ZmASR7-1* were up-regulated at 12 h and stable in control leaves and roots (Fig. 2, B and D). These expression data might be due to the memory of a circadian cycle. In response to ABA treatment, we found that in leaves, transcript levels of *ZmASR5* were down-regulated, while those of *ZmASR1*, *ZmASR3*, and *ZmASR4* were up-regulated (Fig. 2B). In roots, up-regulation by ABA appeared a common fea-

ture to *ZmASR1*, *ZmASR2*, *ZmASR4*, and *ZmASR7-1* (Fig. 2D). Supplying Glc barely altered *ZmASR1* transcript levels in leaves (Fig. 2C). In contrast, in roots, up-regulation by Glc appeared a common feature to *ZmASR1* and *ZmASR5* (Fig. 2E). This Glc response was unlikely to be due to an osmotic effect, since the PEG treatment, at an equal osmotic potential, had no effect on both *ZmASR1* and *ZmASR5* expression (Fig. 2E). Nevertheless, supplying PEG decreased *ZmASR5* transcript levels in leaves as well as *ZmASR2* and *ZmASR7-1* transcript levels in roots (Fig. 2, C and E).

ZmASR1 Is the Primary Detectable ZmASR Protein Responding to Water Deficit in Leaves

Expression at the transcript level is not always reflected at the protein level, so we combined separation of soluble proteins by two-dimensional gel electrophoresis (2-DE) with quantitative analysis of silver-stained gels and identification by liquid chromatography-tandem mass spectrometry (LC-MS/MS) to investigate the protein expression pattern of the ZmASR proteins in ear leaf and kernel tissues harvested at different DAPs from plants subjected to water deprivation 7 d before pollination. Our 2-DE condition allowed the analysis of five ZmASRs (ZmASR1, ZmASR2, ZmASR3, ZmASR4, and ZmASR5), the pI of the remaining ZmASRs (ZmASR6, ZmASR7-1, ZmASR7-2, and ZmASR7-3) being higher than that of the immobilized pH gradient strips used. 2-DE analysis revealed ZmASR1, ZmASR2, and ZmASR3 in ear leaves (Fig. 3, A–G) and only ZmASR1 in kernels (Fig. 3, I–K). A gel-free analysis, which has the advantage of being independent of the protein pI, gave the same results (data not shown). Interestingly, ZmASR1, encoded by one of the most highly expressed *ZmASR* genes, was the most abundant detected ZmASR isoform (Fig. 3H). Under well-watered conditions, its expression was rather stable during the early phase in kernels (Fig. 3H), paralleling the slight decrease observed at the transcript levels only after 7 DAP (Fig. 2G). Under water deficit conditions, its expression gradually increased in ear leaves (Fig. 3H), while it did not show any significant change in kernels (Fig. 3L). In contrast, ZmASR2 showed a relatively moderate increase in ear leaves in response to water deficit, while ZmASR3 did not show any change (Fig. 3H). These data suggest that *ZmASR1* encodes the major ASR isoform for water stress responses in maize.

Ectopic Expression of *ZmASR1* Maintains Kernel Yield under Water-Limited Conditions

To address *ZmASR1* function, transgenic maize plants overexpressing the *ZmASR1* coding sequence (*ZmASR1*-OE) under the control of the constitutive cassava vein mosaic virus promoter (Verdaguer et al., 1998) were generated. After selection and regeneration, followed by two backcrosses with the maize line F2, nine independent hemizygous lines that carried a unique T-DNA insertion and expressed ZmASR1 protein (data not shown) and their wild-type sister lines were selected and evaluated in a field site under well-watered and water-limited conditions (see "Materials and Methods"; Supplemental Fig. S2, A and B). qRT-PCR experiments on leaf 11 (below the ear leaf) 5 d before silk emergence showed that transgenic lines expressed *ZmASR1* about 13- and 4-fold more than wild-type lines under well-watered and water-limited conditions, respectively (Supplemental Fig. S2C). An across-event analysis demonstrated that *ZmASR1*-OE plants exhibited a significant 3% and 4% increase in ear leaf area relative to wild-type plants under both well-watered and water-limited stress conditions, respectively, and a significant 12% increase in shoot biomass yield in well-watered conditions (Fig. 4, A and B; Supplemental Table S5). *ZmASR1*-OE plants also demonstrated an increase ($P < 0.10$) in dry leaf weight and total chlorophyll content under both well-watered and water-limited stress conditions (Supplemental Table S5). Mean yield of wild-type plants at the water deficit block was 2.5 tons ha^{-1}, representing an approximately 43% reduction in yield compared with wild-type plants under well-watered conditions (Fig. 4C; Supplemental Table S5). Yield averages of *ZmASR1*-OE plants as a group were significantly greater than in wild-type plants, by 7% and 17% under well-watered and water-limited conditions, respectively (Fig. 4, C and D; Supplemental Table S5). Together, these results provided evidence that ectopic expression of *ZmASR1* improved and maintained maize kernel yield under well-watered and water-limited conditions in the field.

Transcriptomic, Proteomic, and Metabolic Adjustments in *ZmASR1*-OE Plants

To obtain additional cues with regard to ZmASR1 function, we used the 46K array constructed by the Maize Oligonucleotide Array Project (http://www.maizearray.org) followed by qRT-PCR experiments, 2-DE, and gas chromatography coupled to time-of-flight MS analysis to contrast the transcriptome, the proteome, and the metabolome, respectively, of *ZmASR1*-OE leaves with that of wild-type leaves 5 d before silk emergence under well-watered and water deficit conditions.

A first gene list of 16 differentially expressed genes was established from the transcriptome comparison between *ZmASR1*-OE and wild-type leaves under both treatment conditions based on $P < 0.01$ by two-way ANOVA and the criterion of a 1.5-fold change in transcript abundance. To confirm the differential expression, qRT-PCR experiments were performed based on the same samples that had been used for the initial microarray analysis. Because it was not possible to design gene-specific primers of sufficient quality for qRT-PCR for five target genes, the list was shortened to 11 candidates. Only three of the 11 potential target genes were significantly affected by *ZmASR1*-OE with opposite effects: (1) up-regulation of MZ00000739 and MZ00024643 by *ZmASR1*-OE under well-watered conditions; (2) down-regulation of MZ00022082 by *ZmASR1*-OE under

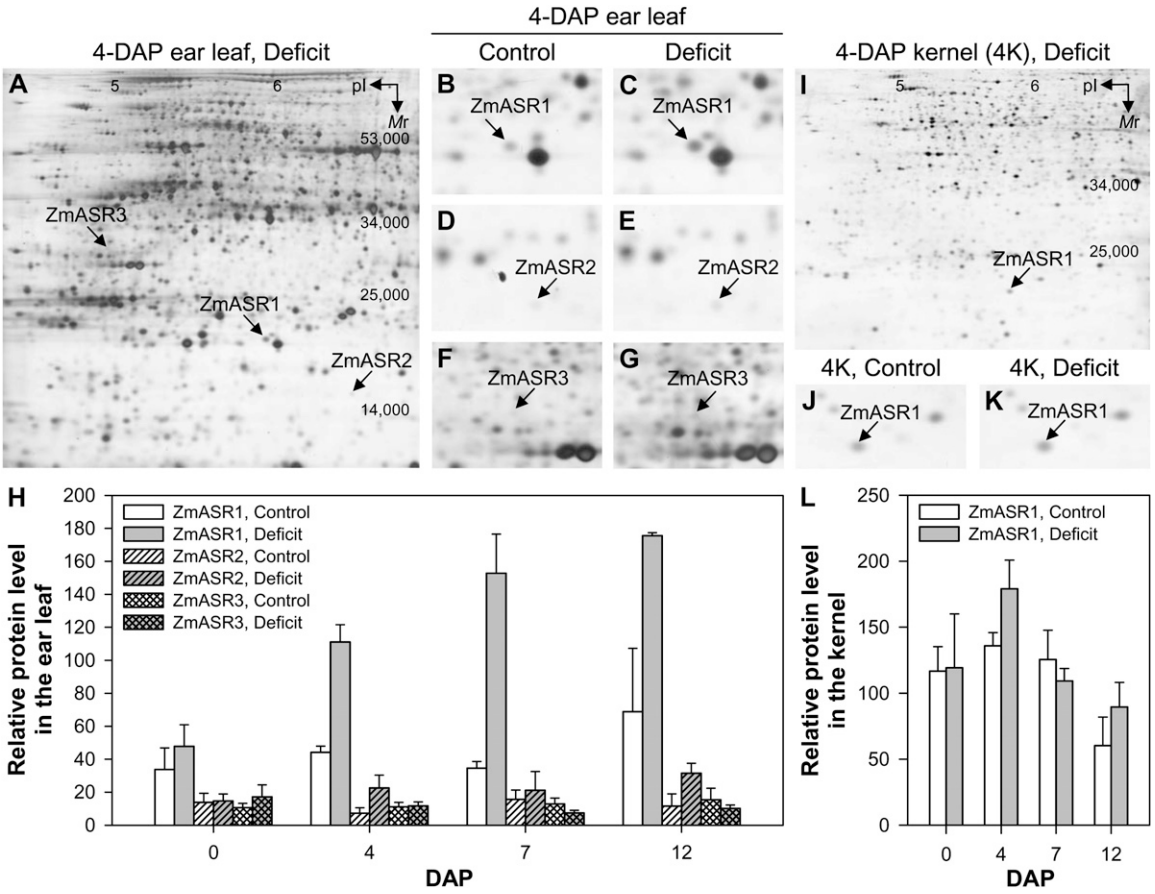

Figure 3. Expression profile of ZmASR1, ZmASR2, and ZmASR3 proteins in ear leaf and kernel tissues. 2-DE gels of ZmASR1, ZmASR2, and ZmASR3 proteins extracted from 0-, 4-, 7-, and 12-DAP ear leaf (150 μg of protein per strip) or kernel (30 μg of protein per strip) of MBS847 plants daily irrigated (control) or subjected to water deprivation (deficit) 7 d before pollination are shown. A to G, 2-DE gel images of 4-DAP ear leaf in well-watered (B, D, and F) and water deficit (A, C, E, and G) conditions with the identified ZmASR1, ZmASR2, and ZmASR3 isoforms. H, Quantification of ZmASR1, ZmASR2, and ZmASR3 isoforms in the ear leaf. I to K, 2-DE gel images of 4-DAP kernel (4K) in well-watered (J) and water deficit (I and K) conditions with the identified ZmASR1 isoform. L, Quantification of the ZmASR1 isoform in the kernel. Values represent means of three biological replicates ± SE.

both well-watered and water deficit conditions (Fig. 5; Supplemental Table S2). MZ00000739 (*ZmSPL14*) likely encoded a nuclear *SQUAMOSA* promoter-binding protein (SBP) box transcription factor of the plant-specific subfamily IIa, most closely related to AtSPL14 from Arabidopsis (Stone et al., 2005; Guo et al., 2008). MZ00022082 encoded a protein with unknown function carrying a WD40 repeat-like-containing domain and was accordingly hereafter named *ZmWD40.1*. Finally, MZ00024643 shared highest identity with *At5g14680* (75%) and *At3g01520* (71%) sequences encoding Arabidopsis vacuolar USPA (for universal stress protein A of *E. coli*) domain proteins (Kerk et al., 2003; Endler et al., 2006) and was accordingly hereafter named *ZmUSPA.1*.

The proteome comparison revealed 22 protein spots that were consistently and significantly more abundant (seven spots) or less abundant (15 spots) in *ZmASR1*-OE leaves than in wild-type leaves in one or both treatment conditions (Table I). Subsequent analyses by LC-MS/MS led to the identification of 16 of them and showed that they were encoded by 15 distinct genes (Table I; Supplemental Table S6). These comprised five up-regulated proteins, annotated as class II aspartyl-tRNA synthetase, β-D-glucosidase, spermidine synthase 1, glucan endo-1,3-β-glucosidase 5, and NAD-dependent epimerase/dehydratase, and 11 down-regulated proteins, annotated as trigger factor-like protein, adenylosuccinate synthetase (two spots encoded by the same gene), plastid transcriptionally active 16, 3-isopropylmalate dehydrogenase (IPMDH; two isoforms, ZmIPMDH1 and ZmIPMDH2), pyruvate dehydrogenase subunit E1β, sedoheptulose-1,7-bisphosphatase, PSII stability/assembly factor, C2-domain containing protein, and thiazole biosynthetic enzyme 1-1. Interestingly, none of the corresponding 15 genes generated expression data with significant *P* value thresholds in the transcriptomic analysis (data not shown).

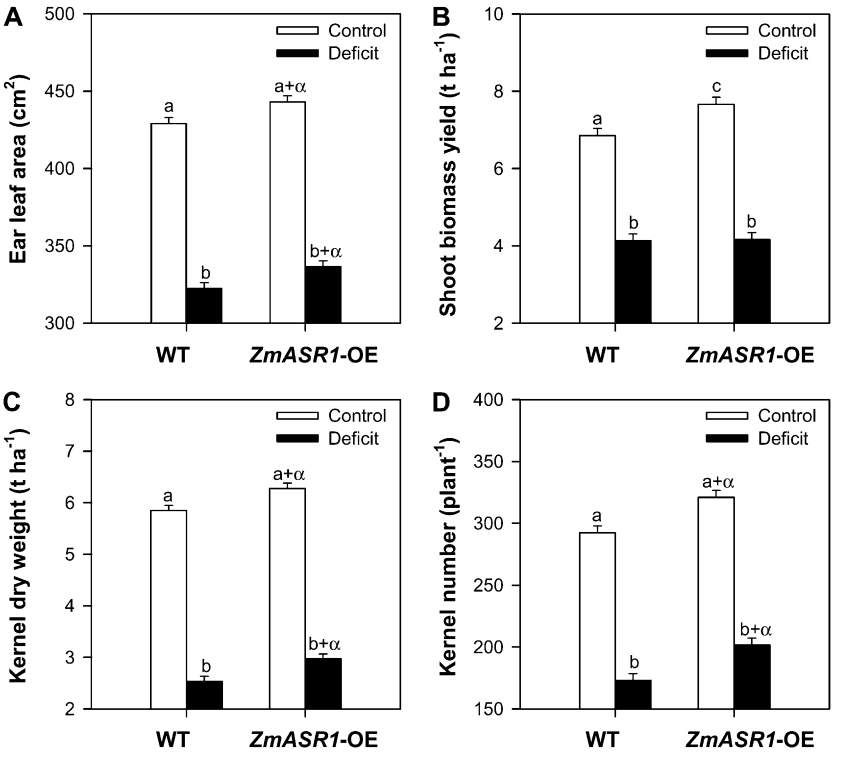

Figure 4. *ZmASR1*-OE plants demonstrate improved vegetative and reproductive performance under water-limiting conditions. Ear leaf area (A), shoot biomass yield (B), kernel dry weight (C), and kernel number (D) values of wild-type (WT) and *ZmASR1*-OE plants are shown for groupings of nine individual *ZmASR1* events. Values are means ± SE (n = 52–60). When two samples show different letters above the bar, the difference between them is significant (normal letters, $P < 0.05$). When both genotype and treatment effects are significant, a, b, a+α, and b+α are indicated (see "Materials and Methods"; and Supplemental Table S5).

Nontargeted metabolite profiling identified 84 unique compounds (Supplemental Table S7). Among them, 20 were consistently and significantly affected by *ZmASR1*-OE with opposite effects: increase in lactate and urea in water deficit conditions and decrease in 18 other metabolites, including 10 amino acids (Ile, Leu, Val, Phe, Trp, Asn, Gln, Pro, Ala, and Gly), two of their derivatives or potential precursors (benzoate and citramalate), and three sugars (galactinol, Glc, and Suc), in both well-watered and water deficit conditions (Table II).

ZmASR1-OE Influences the Expression of Additional BCAA- and Pro-Related Target Genes and a Specific Combination of Metabolites

Since the decrease in the three BCAAs Ile, Leu, and Val was in reasonable agreement with that of the ZmIPMDH1 and ZmIPMDH2 isoforms involved in Leu biosynthesis (Fig. 6), we hypothesized that ZmASR1 could regulate the transcription of key genes involved in drought-responsive pathways that were modified by *ZmASR1*-OE. Therefore, we identified those genes in the maize genome based on sequence homology to Arabidopsis genes and examined the expression level of 32 of them in wild-type and *ZmASR1*-OE leaves by qRT-PCR experiments (Fig. 6; Supplemental Fig. S3; Supplemental Table S2; The Arabidopsis Information Resource and AraCyc; Fang et al., 1992; Taji et al., 2002; Martin et al., 2006; Less and Galili, 2008; Urano et al., 2009). We did not find evidence for transcriptional regulation of *ZmIPMDH1* and *ZmIPMDH2/3* genes, in agreement with the transcriptomic analysis (Supplemental Fig. S3). However, three other BCAA-related transcripts, one for acetohydroxyacid synthase (*ZmAHAS1*) and two for ketolacid reductoisomerase (*ZmKAR1* and *ZmKARI2*), showed significant increases in *ZmASR1*-OE leaves in comparison with wild-type leaves under well-watered conditions (Fig. 6). Furthermore, one transcript for branched-chain aminotransferase (*ZmBCAT4*; BCAA biosynthesis) and two transcripts for Δ^1-pyrroline-5-carboxylate synthetase (*ZmP5CS2* and *ZmP5CS3*; Pro biosynthesis) were up-regulated under both treatment conditions, while another branched-chain aminotransferase paralog (*ZmBCAT2*) was down-regulated in *ZmASR1*-OE leaves under both treatment conditions ($P < 0.10$; Fig. 6; Supplemental Fig. S3). These seven biosynthetic genes were induced in response to water deficit, but only one, *ZmBCAT2*, had an expression pattern consistent with the metabolic changes in *ZmASR1*-OE leaves compared with wild-type leaves (Fig. 6).

To provide further insight into the impact of *ZmASR1*-OE on the transcriptome, proteome, and metabolome of the maize leaf, a within-group correlation matrix analysis was performed. Among 10,153 pairwise correlations computed between 36 transcripts (*ZmASR1*, *ZmSPL14*, *ZmWD40.1*, *ZmUSPA.1*, and the 32 genes related to metabolic pathways modified by *ZmASR1*-OE), 22 protein spots, the total chlorophyll content, and 84 metabolites, we obtained 765, 170, and 23 individual significant correlations at $P < 0.05$, $P < 0.01$, and $P < 0.001$, respectively (Supplemental Tables S8 and S9).

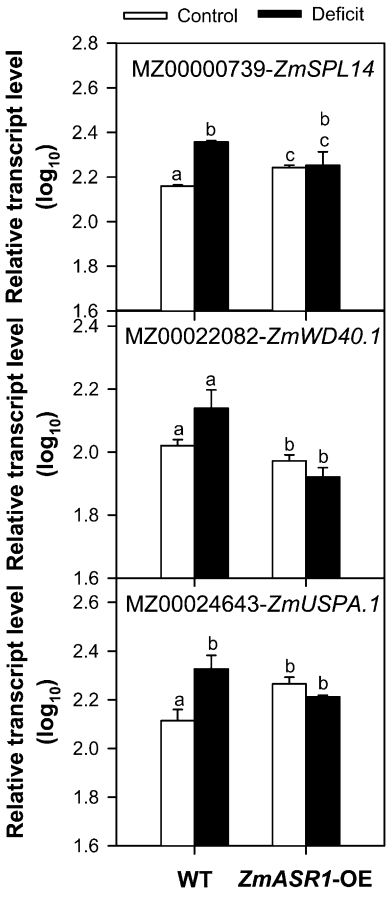

Figure 5. Transcript levels of confirmed ZmASR1 target genes identified by microarray. qRT-PCR was performed on total RNA prepared from the 11th leaves of wild-type (WT) and *ZmASR1*-OE plants that had been used for the initial microarray analysis using gene-specific primers (Supplemental Table S2). Transcript levels were normalized against the stable endogenous *ZmGRP2* gene and shown relative to *ZmBCAT2* transcript levels in the 11th leaf in well-watered (control) conditions. Values represent means of biological duplicates ± SE. When two samples show different letters above the bar, the difference between them is significant (normal letters, $P < 0.05$).

These numbers were nearly twice that expected under the null hypothesis (Supplemental Table S9). Furthermore, the number of positive and negative individual significant correlations did not follow a symmetric binomial distribution (Supplemental Table S9). Similar differences were observed for the transcript-transcript, metabolite-metabolite, and transcript-metabolite submatrices, suggesting that the individual significant correlations obtained for these submatrices were most likely valuable (Supplemental Table S9). The analysis of the metabolite-metabolite submatrix revealed that 13 of the 18 metabolites that were less abundant in *ZmASR1*-OE leaves than in wild-type leaves showed high positive correlation to each other (Table III). Interestingly, six of them were previously reported to be negatively correlated to biomass in Arabidopsis (Table III; Meyer et al., 2007; Sulpice et al., 2009). Furthermore, six others showed high positive correlation with metabolites negatively correlated to biomass in Arabidopsis (Table III; Meyer et al., 2007; Sulpice et al., 2009). The analysis of the transcript-metabolite submatrix showed that ZmASR1 target transcripts involved in BCAA biosynthesis were positively correlated with each other and/or BCAAs and revealed a close link between six ZmASR1 target transcripts (*ZmBCAT4*, *ZmKARI2*, *ZmP5CS2*, *ZmP5CS3*, *ZmUSPA.1*, and *ZmWD40.1*) and the specific combination of 13 decreased metabolites (Supplemental Tables S10 and S11).

DISCUSSION

Expression of *ASR* Genes in Response to Water Deficit in Maize and Other Poaceae Species

Here, we identified nine *ASR* genes in the maize genome, making the *ZmASR* gene family the biggest *ASR* gene subfamily identified to date. Phylogenetic analyses indicated several duplication events after the divergence of Liliales from Commelinids, giving rise to five paralogous clades of *ASR* genes in the Poaceae family. Anchoring of the *ASR* genes on the maize physical map shows that all Poaceae sequences can be assigned to one of the Poaceae ancestor protochromosomes previously defined by Salse et al. (2008). Thus, sequences from the subclades I-1, I-2, I-3, II-1, and II-2 trace back to chromosomes A11/A12, A4, A1, A2/A4, and A1, respectively. Consequently, the data support the idea that the Poaceae intermediate ancestor with 12 protochromosomes (Murat et al., 2010) already had seven *ASR* genes. The sequence of events raising this small gene family in grasses might have taken place during the diploidization process following the Poaceae-specific whole-genome duplication (Murat et al., 2010). A larger sample of sequence data from monocots other than Poaceae might help to further elucidate this point.

Our gene-specific qRT-PCR expression data combined with 2-DE analysis and the recent work of Philippe et al. (2010) in rice strongly suggest that members of the Poaceae subclade I-1, including *ZmASR1* and *OsASR5*, are the most prevalent ASR proteins in major plant tissues. It is noteworthy that recently released large-scale quantitative proteomics studies only revealed ZmASR1 and ZmASR2 in maize leaves (Friso et al., 2010; Majeran et al., 2010). In C_4 Poaceae species, such as maize, a key component of mature leaves is the partitioning of photosynthetic processes between the bundle sheath and the mesophyll. Among the 25,800 transcripts (about 80% of the predicted maize transcriptome) that were revealed along the maize leaf gradient, Li et al. (2010) identified only five (*ZmASR1*, *ZmASR2*, *ZmASR3*, *ZmASR4*, and *ZmASR5*) of the nine *ZmASR* genes characterized in this study. It is striking that they all belong to the suite of genes (21%) that were determined to be differentially expressed between bundle sheath and mesophyll cells (Li et al., 2010). Thus, *ZmASR4* showed enriched expression in bundle sheath

Table I. *Proteins that showed significant changes in ZmASR1-OE leaves compared with wild-type leaves*

Spot ID[a]	Trend in *ZmASR1*-OE	Ratio of *ZmASR1*-OE to the Wild Type[b]		ANOVA Table[c]			Maize Gene Model[d]	Annotation[e]	Class
		Control	Deficit	*ZmASR1*-OE	Deficit	Interaction			
s0732	Down	0.99	0.34	NR	NR	*0.007*	NI	ND	ND
s1021	Up	1.30	2.22	**0.020**	0.752	0.071	GRMZM2G019121	Class II aspartyl-tRNA synthetase (AspRS)	Amino acid activation
s1202	Up	2.94	1.74	**0.020**	0.420	0.561	GRMZM2G008247	β-D-Glucosidase (GLU)	Carbohydrate metabolism
							GRMZM2G034152	*Flavin-containing amine oxidase*	
s1388	Down	0.50	0.55	**0.006**	0.304	0.578	GRMZM2G127393	Trigger factor-like protein	Protein folding
s1406	Down	0.13	0.73	NR	NR	*0.027*	GRMZM2G123204	Adenylosuccinate synthetase (AdSS)	Purine biosynthesis
							GRMZM2G020446	*Diaminopimelate decarboxylase*	
s1422	Down	0.42	0.98	NR	NR	0.031	GRMZM2G123204	Adenylosuccinate synthetase (AdSS)	Purine biosynthesis
s1442	Down	0.26	0.56	**0.015**	0.491	0.118	NI	ND	ND
s1444	Down	0.66	0.74	**0.005**	0.289	0.686	GRMZM2G449496	Plastid transcriptionally active 16 (PTAC16)	RNA regulation
s1612	Down	0.37	0.86	NR	NR	*0.001*	GRMZM2G104613	3-Isopropylmalate dehydrogenase 2 (IPMDH2)	Leu biosynthesis
							GRMZM2G803490	*3-Isopropylmalate dehydrogenase 1 (IPMDH1)*	
s1641	Down	0.48	0.88	NR	NR	*0.026*	GRMZM2G803490	3-Isopropylmalate dehydrogenase 1 (IPMDH1)	Leu biosynthesis
s1886	Down	0.68	0.65	**0.019**	0.248	0.953	GRMZM2G097226	Pyruvate dehydrogenase subunit E1β (PDH-E1β)	Glycolysis and tricarboxylic acid cycle
s1904	Down	0.70	0.63	**0.007**	0.017	0.859	AC147602.5_FGP004	Sedoheptulose-1,7-bisphosphatase (SBPase)	Calvin cycle
s1913	Down	1.14	0.68	NR	NR	*0.001*	GRMZM2G102838	PSII stability/assembly factor (HCF136)	Protein assembly
s2020	Down	0.99	0.50	NR	NR	*0.010*	AC210204.3_FGP002	C2 domain-containing protein	Stress
s2141	Down	0.30	0.68	**0.005**	0.035	0.150	NI	ND	ND
s2210	Down	0.71	0.38	**0.019**	0.215	0.258	GRMZM2G018375	Thiazole biosynthetic enzyme 1-1 (THI1)	Thiamine biosynthesis
s2275	Up	1.82	1.23	**0.050**	0.013	0.055	GRMZM2G064163	Spermidine synthase 1	Polyamine biosynthesis
s2316	Up	1.56	1.29	**0.011**	0.028	0.133	GRMZM2G078566	Glucan endo-1,3-β-glucosidase 5	Carbohydrate metabolism
s2322	Up	1.75	1.34	**0.005**	0.436	0.108	NI	ND	ND
s2460	Down	0.82	0.63	**0.035**	0.023	0.112	NI	ND	ND
s2528	Up	1.54	1.21	**0.020**	0.778	0.244	GRMZM2G068244	NAD-dependent epimerase/dehydratase	Coenzyme binding
s3353	Up	1.85	1.32	**0.020**	0.306	0.170	NI	ND	ND

[a]Identification number of the corresponding protein spot on the two-dimensional reference map. [b]The expression values are reported relative to the wild-type samples in the same culture condition ($n = 2$). [c]Proteins were categorized as *ZmASR1*-OE (boldface text), deficit (underlined text), and interaction (italicized text) as follows: *ZmASR1*-OE, proteins that showed significant ($P < 0.05$) changes in *ZmASR1*-OE leaves compared with wild-type leaves when the additive model could be retained; deficit, proteins that showed significant ($P < 0.05$) changes under water deficit conditions compared with well-watered conditions when the additive model could be retained; interaction, proteins that showed significant ($P < 0.05$) changes in *ZmASR1*-OE leaves compared with wild-type leaves by the Bonferroni method when the additive model could not be retained. Experimental details are described in "Materials and Methods." NR, Not relevant. [d]Maize genome release 5a.59 of November 2010 (http://www.maizesequence.org). NI, Not identified by LC-MS/MS. [e]Manually improved annotation from SwissProt, GenBank, Trembl, and InterPro databases. Annotations in italicized text were eliminated based on the absence of correspondence between the theoretical M_r and the observed M_r and/or the protein abundance index (see Supplemental Table S6). ND, Not determined.

Table II. *Metabolites that showed significant changes in ZmASR1-OE leaves compared with wild-type leaves*

Pathway	Metabolite	Trend in *ZmASR1*-OE	Ratio of *ZmASR1*-OE to the Wild Type[a]		ANOVA Table[b]		
			Control	Deficit	*ZmASR1*-OE	Deficit	Interaction
BCAAs	Ile	Down	−0.11	−0.15	**0.010**	0.014	0.573
	Leu	Down	−0.08	−0.14	**0.007**	0.002	0.284
	Val	Down	−0.09	−0.11	**0.010**	0.143	0.790
Aromatic amino acids	Phe	Down	−0.06	−0.12	**0.011**	0.001	0.189
	Trp	Down	−0.11	−0.16	**0.016**	0.014	0.583
Glu family	Asn	Down	−0.13	−0.20	**0.044**	0.170	0.624
	Gln	Down	−0.07	−0.12	**0.037**	0.006	0.550
	Pro	Down	−0.06	−0.08	**0.032**	0.003	0.783
RFO	Galactinol	Down	−0.13	−0.08	**0.010**	0.000	0.415
Saccharides	Glc	Down	−0.17	−0.08	**0.004**	0.000	0.221
	Suc	Down	−0.14	−0.08	**0.037**	0.277	0.505
γ-Aminobutyrate shunt	Ala	Down	−0.08	−0.09	**0.024**	0.012	0.856
Others	trans-Aconitate	Down	−0.22	−0.10	**0.021**	0.183	0.280
	Benzoate	Down	−0.09	−0.11	**0.039**	0.173	0.833
	trans-Caffeoylquinate	Down	−0.13	−0.16	**0.033**	0.078	0.781
	Citramalate	Down	−0.10	−0.19	**0.040**	0.005	0.434
	Gly	Down	−0.11	−0.11	**0.005**	0.005	0.968
	Lactate	Up	0.31	1.81	NR	NR	*0.045*
	Monomethylphosphate	Down	−0.16	−0.21	**0.004**	0.020	0.551
	Urea	Up	0.37	1.23	NR	NR	*0.042*

[a]Values ($\log_{10}$) are reported relative to the wild-type samples ($n = 2$). [b]Metabolites were categorized as *ZmASR1*-OE (boldface text), deficit (underlined text), and interaction (italicized text) as follows: *ZmASR1*-OE, metabolites that showed significant ($P < 0.05$) changes in *ZmASR1*-OE leaves compared with wild-type leaves when the additive model could be retained; deficit, metabolites that showed significant ($P < 0.05$) changes under water deficit conditions compared with well-watered conditions when the additive model could be retained; interaction, metabolites that showed significant ($P < 0.05$) changes in *ZmASR1*-OE leaves compared with wild-type leaves under water deficit conditions by the Bonferroni method when the additive model could not be retained. Experimental details are described in "Materials and Methods." NR, Not relevant.

cells, in agreement with a previous work that used differential screening analysis (Furumoto et al., 2000), while *ZmASR1*, *ZmASR2*, *ZmASR3*, and *ZmASR5* showed enriched expression in mesophyll cells. Such a pattern of expression suggests that the *ZmASR* gene family shows subfunctionalization. Interestingly, almost all Poaceae sequences in subclades I-1, I-2, and II-2, including *ZmASR1*, *ZmASR2*, *ZmASR3*, *ZmASR7-2*, and *ZmASR7-3*, share a putative nuclear localization signal and substantial sequence identity with the Zn^{2+}-dependent DNA-binding activity domain of LLA23 and SlASR1 proteins, raising the interesting possibility that the ASR proteins belonging to these subclades act as regulators modulating gene expression. Unlike the other members of the maize *ASR* gene family, *ZmASR7-1*, *ZmASR7-2*, and *ZmASR7-3* do not contain any introns. Because *ZmASR7-1* was expressed at a low level, whereas the expression of *ZmASR7-2* and *ZmASR7-3* was not determined by qRT-PCR, conventional RT-PCR was used to monitor the transcript levels of *ZmASR7-2* and *ZmASR7-3* and to rule out the possibility that these genes might be pseudogenes. Both transcripts were detected in leaf and root tissues, although at very low levels, regardless of the water stress-related conditions (Supplemental Fig. S4).

Additionally, our transcript and protein expression data confirmed and extended findings of up-regulation by water deficit of *ZmASR1* in maize leaves (Riccardi et al., 1998, 2004). Indeed, we showed up-regulation of *ZmASR1*, *ZmASR2*, *ZmASR4*, and *ZmASR7-1* by water deficit in leaves, although direct treatment with ABA in leaves induced elevations of *ZmASR1*, *ZmASR3*, and *ZmASR4*. Up-regulation by water deficit and ABA treatment was previously shown for the sugarcane and rice *ZmASR1* orthologs *SoDIP22* and *OsASR5* (Sugiharto et al., 2002; Rabbani et al., 2003; Takasaki et al., 2008). These data indicate that members of the Poaceae subclade I-1, except *ZmASR2*, may play important roles in ABA-dependent pathways in the water deficit response in Poaceae leaves. In contrast, *ZmASR2* and *ZmASR7-1* are regulated by ABA-independent pathways under water deficit in mature leaves, as reported previously for potato *DS2* genes (Silhavy et al., 1995; Doczi et al., 2002). It is worth noting that maize and rice (Philippe et al., 2010) *ASR* genes belonging to Poaceae subclades I-3 (*ZmASR4* and *OsASR6*) and II-2 (*ZmASR7-1* and *OsASR1*) were all up-regulated by water deficit in mature leaves. In contrast, maize and rice *ASR* genes belonging to Poaceae subclades I-2 (*ZmASR3* and *OsASR4*) and II-1 (*ZmASR5* and *OsASR3*) were not significantly altered and down-regulated by water deficit in mature leaves, respectively. Therefore, these data suggest that the *ASR* expression in response to water deficit represents an evolutionarily conserved regulatory mechanism in the Poaceae and several unrelated eudicot plants. A better understanding of the physiological roles of the maize *ASR* genes will require more exhaustive defini-

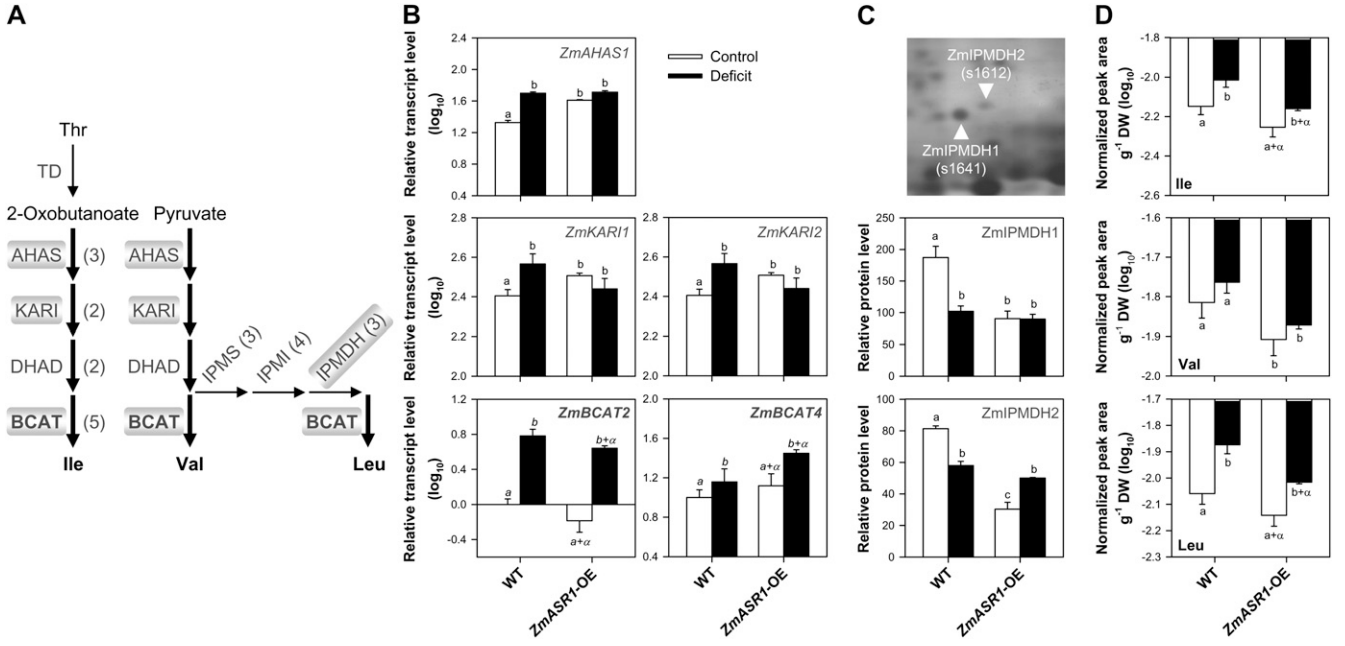

Figure 6. *ZmASR1*-OE influences BCAA-related gene expression and BCAA composition. A, The BCAA biosynthetic pathway. Substrates and products are in lightface and boldface text, respectively. Enzymes are in gray, and the number of isoforms identified in maize is indicated in parentheses. The enzymes in boldface are the rate-limiting enzymes during the water deficit response. Thick arrows indicate common steps in BCAA biosynthesis. Enzymes in boxes are ZmASR1 targets. B to D, Relative transcript (B), protein (C), and metabolite (D) levels in the 11th leaves of wild-type (WT) and *ZmASR1*-OE plants according to Figure 5, Table I, and Table II. Values represent means of biological duplicates ± SE. When two samples show different letters above the bar, the difference between them is significant (roman letters, $P < 0.05$; italic letters, $P < 0.10$). When both genotype and treatment effects are significant, a, b, a+α, and b+α are indicated (see "Materials and Methods"). AHAS, Acetohydroxyacid synthase; DHAD, dihydroxyacid dehydratase; DW, dry weight; IPMI, isopropylmalate isomerase; IPMS, isopropylmalate synthase; TD, Thr deaminase.

tion of their expression profiles in response to water deficit at the cellular level. It would also be important to determine whether these genes are affected by water deficit at the posttranslational level.

ZmASR1 Maintained Kernel Yield under Water Deficit Conditions through a Set of Low-M_r Metabolites Related to Growth Rate

ASR overexpression studies in plants are exemplified by works carried out on Solanoideae (Kalifa et al., 2004b; Frankel et al., 2007) and Arabidopsis, although the latter does not include any *ASR* homologous genes (Yang et al., 2005; Liu et al., 2010). Our study demonstrated that *ZmASR1*-OE improved the kernel yield of transgenic maize in the field under well-watered and water-limited conditions. The positive yield impact of *ZmASR1* was both on kernel number and weight. These results were unexpected based on our previous PQL study, which did not reveal any QTL for maize yield and its component in the vicinity of the *ZmASR1* chromosomal region (de Vienne et al., 1999; Jeanneau et al., 2002). Nevertheless, it may be pointed out that recently identified QTLs for ear length under water-stressed conditions (Lu et al., 2006) and female flowering time (Marino et al., 2009) are centered on the *ZmASR1* locus. The finding that *ZmASR1*-OE plants demonstrated significant improvements in ear leaf area and shoot biomass yield, as well as increases in leaf dry weight and total chlorophyll content, implies that these improvements in vegetative productivity translated into improvements in reproductive performance and kernel yield. Enhanced vegetative tolerance under well-watered conditions is surprising, as we would have expected no significant differences, as described previously under mild water deficit conditions (Jeanneau et al., 2002). Nevertheless, transgenic maize plants overexpressing *ZmNF-YB2* were darker green and flowered 1 to 3 d earlier than the control plants under conditions of ample water supply (Nelson et al., 2007). Additionally, enhanced vegetative tolerance and improved kernel yield under water deficit conditions were produced by the overexpression of *ZmNF-YB2*, *betA*, or *Csp* genes in maize (Quan et al., 2004; Nelson et al., 2007; Castiglioni et al., 2008). Continued evaluation of *ZmASR1*-OE across different hybrid genetic backgrounds adapted for the marketplace will be important ongoing work. Furthermore, testing the ability of other water deficit-inducible *ZmASR* genes for their ability to confer water deficit tolerance will further define the structure-function relationships and

Table III. *Pairwise correlations of ZmASR1 target metabolites against decreased and/or biomass-related metabolites*

Pathway	Parameter x[a]	Trend in *ZmASR1*-OE	Parameter y[b]	Correlation (x,y)[c]
Glu family	Gln	Down	Leu	−0.8897
BCAAs	Leu	Down	***Gln***	−0.8897
	Ile	Down	Leu	0.9708
	Val	Down	***Phe***	0.9188
			Pro	0.9935
Aromatic amino acids	Phe	Down	***Val***	0.9188
			Pro	0.9319
Glu family	Pro	Down	***Phe***	0.9319
			Val	0.9935
RFO	Galactinol	Down	***Benzoate***	0.9598
			Citrate	0.9371
			Monomethylphosphate	0.8921
			Raffinose	0.8893
			Succinate	0.9280
			Threonate	0.9378
Saccharides	Glc	Down	trans-Aconitate	0.9409
			Ala	0.9330
			Ascorbate	0.8875
			trans-Caffeoylquinate	0.9264
			Citramalate	0.9457
			Malate	0.9564
			Suc	0.9006
	Suc	Down	***Ascorbate***	0.9692
			trans-Caffeoylquinate	0.9532
			Citrate	0.9587
			Ethanolamine	0.8896
			Glc	0.9006
			Malate	0.9466
			Orn	0.9113
γ-Aminobutyrate shunt	Ala	Down	trans-Aconitate	0.9643
			Citramalate	0.9656
			Glc	0.9330
			Malate	0.9579
Others	trans-Aconitate	Down	***Ala***	0.9643
			Citramalate	0.9669
			Glc	0.9409
			Malate	0.9118
			Raffinose	0.8973
	Benzoate	Down	Galactinol	0.9598
			Monomethylphosphate	0.8797
			Raffinose	0.8909
			Threonate	0.8848
	trans-Caffeoylquinate	Down	***Ascorbate***	0.9735
			Ethanolamine	0.9181
			Glc	0.9264
			Malate	0.8884
			Suc	0.9532
	Citramalate	Down	trans-Aconitate	0.9669
			Ala	0.9656
			Glc	0.9457
			Malate	0.8958
	Monomethylphosphate	Down	***Benzoate***	0.8797
			Galactinol	0.8921
			Raffinose	0.9420

[a]Metabolites that showed significant changes in *ZmASR1*-OE leaves compared with wild-type leaves ($P < 0.05$). [b]Metabolites that showed significant decreases in *ZmASR1*-OE leaves compared with wild-type leaves and/or were correlated to biomass in Arabidopsis (Meyer et al., 2007; Sulpice et al., 2009). Boldface italic type and underlined lightface italic type distinguish metabolites negatively and positively correlated to biomass, respectively, in Arabidopsis (Meyer et al., 2007; Sulpice et al., 2009). [c]Correlations were calculated from residual data ($P < 0.05$). The original data are in Supplemental Table S8.

improve our understanding of the mode of action of the ZmASR proteins.

A noteworthy observation from our data is that 18 low-M_r metabolites decrease in mature *ZmASR1*-OE leaf. Of high relevance are 12 standard or related amino acids and three sugars: (1) Ala, which is synthesized from pyruvate; (2 and 3) Asn and Gln, which are the central regulators of carbon/nitrogen metabolism; (4) Gly, whose metabolism occurs by several different pathways, including Thr catabolism; (5–7) Ile (Thr-derived pathway) and the two other BCAAs, Leu and Val (pyruvate-derived pathway), that show the highest hydrophobicity among the proteinogenic amino acids and are accordingly the major constituents of transmembrane regions of membrane proteins; (8 and 9) Phe and Trp, whose synthesis initiates from chorismate and that serve in plants as precursors for a wide range of secondary metabolites having multiple functions; (10) Pro, which is synthesized from either Glu or Orn and has multiple functions in stress adaptation, recovery, and signaling; (11) benzoate, which derives from Phe and is a precursor to several important benzenoid compounds, including the defense signaling compound salicylic acid; (12) citramalate, which may serve as a precursor for Ile biosynthesis in plants as in microorganisms (de Kraker et al., 2007; Joshi et al., 2010; Less et al., 2010; Szabados and Savouré, 2010); (13) Suc, which is the major end product of photosynthesis and the major transport form of carbon from source and sink; (14) its cleavage product Glc, which enhances the expression of genes implied in carbohydrate metabolism (Koch, 1996; Trouverie et al., 2004); (15) galactinol (raffinose family oligosaccharide [RFO]), which plays a novel role in the protection of cellular metabolism, in particular, the photosynthesis of chloroplast, from oxidative damage caused by several types of abiotic stresses (Nishizawa et al., 2008). Our finding that *ZmASR1*-OE triggers an adjustment in the Glc level is in good agreement with the observation that a QTL for hexose content colocates with the *ZmASR1* locus (Pelleschi et al., 2006) and a previous report in potato in which *SlASR1* was overexpressed (Frankel et al., 2007). Additionally, the lower levels of Pro in *ZmASR1*-OE plants is in close agreement with previous reports in tobacco and potato plants in which *SlASR1* was overexpressed and down-regulated, respectively (Kalifa et al., 2004b; Frankel et al., 2007). Lower levels of Phe, Val, and Suc had also been described for potato plants overexpressing *SlASR1* (Frankel et al., 2007), although the remaining other decreased metabolites had never been identified before. Interestingly, among the 18 decreased metabolites, 13 were positively correlated to each other. Previous reports documented that biomass can be predicted by a specific metabolite status (Meyer et al., 2007; Sulpice et al., 2009). It is intriguing that among the 13 positively correlated metabolites, six (Ala, Phe, Val, Suc, benzoate, and citramalate) were previously shown to be negatively correlated to biomass (Meyer et al., 2007; Sulpice et al., 2009). It is also noteworthy that six others (transaconitate, transcaffeoylquinate, galactinol, Glc, monomethylphosphate, and Pro) showed positive correlation to metabolites negatively correlated to biomass (Meyer et al., 2007; Sulpice et al., 2009). Additionally, it was found that Pro levels accumulated under water deficit conditions were negatively correlated with maize yield (Udomprasert et al., 1999). Since *ZmASR1*-OE plants demonstrated improvement and maintenance in shoot biomass yield under well-watered and water-limited conditions, respectively, as well as decreases in this specific set of 13 metabolites under both treatment conditions, we hypothesize that ZmASR1 might negatively impact the level of these 13 metabolites, which would contribute to biomass yield and subsequently result in improvements and maintenance of kernel yield under well-watered and water deficit conditions, respectively.

Influence of ZmASR1 on the Expression of Genes Involved in BCAA Biosynthesis

What is the relationship between ZmASR1 and the level of these 13 metabolites that may impact on biomass and kernel yield? Our global comparative study led to the identification of 25 genes that were either transcriptionally (10 genes) or posttranscriptionally (16 proteins encoded by 15 distinct genes) up-regulated (eight transcripts and five proteins) or down-regulated (two transcripts and 11 proteins) by *ZmASR1*-OE in mature leaves. Three-quarters of them encoded proteins normally localized in plastids or accumulating in these organelles under osmotic stress and involved in primary metabolic pathways. Importantly, the microarray analysis and the additional qRT-PCR experiments revealed different target genes from the proteomic analysis. Therefore, the two approaches were complementary. It is quite evident that some genes with transcript changes in *ZmASR1*-OE leaves compared with wild-type leaves might not have been revealed by the proteomic analysis because of their low abundance. Nevertheless, none of the 16 identified proteins that showed substantial changes in abundance in *ZmASR1*-OE leaves compared with wild-type leaves were transcriptionally regulated in *ZmASR1*-OE leaves. This is not necessarily surprising, since it has been shown recently that posttranscriptional regulation can affect the protein abundance without affecting transcript levels (Böhmer and Schroeder, 2011). These data, therefore, strengthen the idea that ZmASR1, similar to other ASR proteins, may act both as a transcriptional regulator and a chaperone-like protein protector (Saumonneau et al., 2008; Urtasun et al., 2010). A synergistic relationship was found between the osmolyte Gly betaine and the SlASR1 protein, suggesting a combined mechanism of action of these two proteins in response to abiotic stresses (Konrad and Bar-Zvi, 2008). However, the enhanced Gly betaine accumulation in transgenic *betA*-overexpressing maize lines led to greater increases in total soluble sugars and

free amino acids (Quan et al., 2004), in contrast to the metabolite effects we report in *ZmASR1*-OE plants. Thus, the mechanism of action of ZmASR1 is likely to be different from that of Gly betaine. Just recently, a wheat (*Triticum aestivum*) group 2 LEA protein named DHN-5, which is closely related to the maize LEA protein RAB17 and involved in salt and osmotic tolerance (Brini et al., 2007), has been shown to enhance the thermostability and activity of β-D-glucosidase (Brini et al., 2010), a target protein of ZmASR1. It is striking that β-D-glucosidase and 12 other ZmASR1 target genes belong to the list of established and potential thioredoxin (Trx) targets (He et al., 2009; Montrichard et al., 2009). Closer analysis shows that seven additional ZmASR1 target genes may contain Cys residues involved in disulfide bridges, making a total of 20 ZmASR1 target genes potentially linked to Trx. Thus, our results open the way to the very speculative hypothesis that ZmASR1 exhibits a chaperone-like activity on selectively redox-regulated proteins.

Among the established and potential Trx targets with expression changes in *ZmASR1*-OE plants, we found seven genes involved in BCAA biosynthesis. A unique feature of BCAA biosynthesis, which seems to occur exclusively in plastids, is that Val and Ile are formed in two parallel pathways using the same enzymes, namely AHAS, KARI, dihydroxyacid dehydratase, and BCAT, while Leu formation branches off from 2-oxoisovalerate, the last intermediates of the Val biosynthetic pathway, to follow a three-step chain elongation catalyzed by isopropylmalate synthase, isopropylmalate isomerase, and IPMDH, which ends with a transamination step catalyzed by a BCAT (Binder et al., 2007; Joshi et al., 2010). Decreases in *ZmBCAT2* transcripts and ZmIPMDH1 and ZmIPMDH2 proteins in *ZmASR1*-OE leaves in comparison with wild-type leaves fit well with the finding that *ZmASR1*-OE triggers significant decreases in BCAAs. Furthermore, transcript levels of *ZmAHAS1*, *ZmKARI1*, *ZmKARI2*, and *ZmBCAT4* were correlated with each other and/or the levels of the specific set of 13 decreased metabolites. Importantly, ZmKARI1 and ZmKARI2 showed enriched expression in mesophyll cells in comparison with bundle sheath cells (Majeran et al., 2005; Friso et al., 2010), similar to that was observed for ZmASR1 (Li et al., 2010). There are contradictory reports in the literature on the distribution of ZmIPMDH1 and ZmIPMDH2 across mesophyll and bundle sheath chloroplasts, with a 2-fold enrichment in either mesophyll (Majeran et al., 2005) or bundle sheath (Friso et al., 2010) chloroplasts. Distribution data for ZmAHAS1, ZmBCAT2, and ZmBCAT4 are as yet unavailable, although it is noteworthy that ZmBCAT1 and ZmBCAT3 showed enriched expression in mesophyll cells (Friso et al., 2010). Additionally, it may be noted that Arabidopsis Trx-m1 is the most effective Trx on AtIPMDH1 in comparison with Arabidopsis Trx-f1 or bacterial Trx (He et al., 2009). Its maize ortholog (Trx-m4) also showed enriched expression in mesophyll cells (Majeran et al., 2005; Friso et al., 2010). Taken together, our data demonstrate the causal relationship between the overexpression of ZmASR1 and genes involved in BCAA biosynthesis and support the idea that the improvement in biomass associated with *ZmASR1*-OE involves the coordinated transcriptional regulation of BCAA biosynthetic genes. The resolution of the other ZmASR1 target genes is severely hampered by the fact that only limited functional information is available on them. In this respect, a noteworthy observation is that Cañas et al. (2010) have just recently shown that increasing the expression of the enzyme P5CS may have a beneficial effect on yield. Additional experiments will be required to reveal the role of the other ZmASR1 gene targets in water deficit tolerance.

MATERIALS AND METHODS

Plant Materials and Cultures

Stress Treatments at the Vegetative Stage

To carry out the water deficit experiment, maize (*Zea mays*) B73 plants grown in a greenhouse (photoperiod of 16 h supplemented with artificial lighting, 25°C/18°C [day/night], and 60%/55% [day/night] relative humidity) with appropriate daily watering (50% soil water content) until the fifth leaf reached a 35-cm length (about 21 d on average) were deprived of water (WDS test) or daily irrigated (50% soil water content; control condition). The fifth and sixth leaves were harvested when growth of the sixth leaf stopped (0.2 cm or less; WDS test) or after 3 d of constant leaf elongation rate (control condition), 5 to 7 h after the onset of the light period. Four-centimeter-long fragments of the sixth leaves and a 10-cm-long fragment from the middle of the fifth leaf blade were immediately frozen in liquid nitrogen. For ABA, Glc, and PEG treatments, we used leaves and roots described in detail by Trouverie et al. (2004). All samples were ground in a 2-mL microcentrifuge tube containing both 5- and 7-mm steel beads for two to three series of 20 s using a TissueLyser II at 20 Hz (Qiagen) and stored at −80°C until analysis.

Stress Treatment at the Reproductive Stage

Tissues used to establish expression profiles during maize ovule and kernel development (−5 to 70 DAP) were described in detail by Massonneau et al. (2005). To carry out the water deficit experiment, maize MBS847 plants were grown in the greenhouse as described by Qin et al. (2004). Seven days before pollination, plants were deprived of water or irrigated daily. Sampling took place at 0, 4, 7, and 12 DAP, 5 to 7 h after the onset of the light period. The ears and 10-cm-long fragments from the bottom thirds of the corresponding axillary leaves were harvested from plants subjected to each treatment. Mature ovules and kernels were collected from the central part of the ears, separated from the adhering perianth and the pedicel, and stored in liquid nitrogen. All plant materials were ground in a mortar in liquid nitrogen and stored at −80°C until analysis.

Stress Treatment and Yield Trial in the Field

To evaluate the *ZmASR1*-OE plants in the field under limited water treatment, nine independently integrated *ZmASR1*-OE events were grown at Magneraud, France, in May 2005 using two randomized block designs (one to four rows per event; 45 plants per row in each block, transgene-positive and transgene-negative plants in each row identified by PCR during the late vegetative stage of development). One block was maintained in a well-watered condition and the other one placed under limited water supply using mobile devices preventing watering by rainfall (Supplemental Fig. S1A) and three sets of two Watermark probes dispatched at the top third, middle third, and bottom third of each block. For each location, there were two probes placed vertically in the soil, 30 and 60 cm below the surface, and connected to a data logger, allowing daily collection of soil water potential data. These data and growth stage of plants were integrated into the "grapher Watermark" software designed for a specific quality of soil, allowing the monitoring of the trial for signs of water deficit throughout the season. Consequently, the limiting-water condition was achieved at the late vegetative stage of devel-

opment (e.g. from 19 d before silk emergence; Supplemental Fig. S1, B and C). Among the nine events, the three with strongest expression of the transgene (two to three rows per event in each block) were selected for further analysis. Two-centimeter-long fragments in the bottom third of the 11th leaves below the ear leaf were collected 57 d after sowing (5 d before silk emergence), 5 to 7 h after the onset of the light period, and immediately frozen in liquid nitrogen. They were then ground in a 2-mL microcentrifuge tube containing both 5- and 7-mm steel beads for two to four series of 20 s, using a TissueLyser II at 20 Hz (Qiagen). Biological duplicates were formed by dividing each row in two groups and pooling the three selected events, without changing the proportion of each row: samples included 46 plants in total, with 14 to 18 plants per event and two to three rows per event. All samples were stored at −80°C until analysis.

Plant Transformation

The plasmid used for the production of *ZmASR1*-OE plants contains the backbone of vector pSB12 (Komari et al., 1996), a Basta resistance cassette (rice *Actin* promoter and intron, *Bar* and *Nos* terminators) next to the right border, and the *ZmASR1* cDNA of maize MBS847 (GenBank accession no. AX297905), under the control of the cassava vein mosaic virus promoter, next to the left border. *Agrobacterium tumefaciens*-mediated transformation of maize inbred line A188 was based on a published protocol (Ishida et al., 1996). For each transformation event, the number of T-DNA insertions was evaluated by Southern blot, the integrity of the transgene was verified by PCR, and the expression level of the transgene was evaluated by RT-PCR and 2-DE as described (Jeanneau et al., 2002; Depège-Fargeix et al., 2011). Seventeen independent transformation events were crossed with the maize inbred line F2, in which the ZmASR1 protein is not detected (Riccardi et al., 1998; Jeanneau et al., 2002). T1 events were then selected and backcrossed one more time with the maize inbred line F2. Among the 17 independently integrated T2 events, the nine with strongest expression of the transgene compared with the endogenous *ZmASR1* gene based on 2-DE were evaluated in the field. In the T2 generation containing 50% transgenics, the wild-type plants were used as control plants.

Database Search, Gene Structure Determination, and Chromosomal Location of *ZmASR* Genes

To search for *ZmASR1* homologs in maize, we used the *ZmASR1* cDNA in BLAST analysis using EST assemblies in The Gene Index database (http://compbio.dfci.harvard.edu/tgi/plant.html), assemblies of genomic DNA fragments at The Plant Genomics Resources (http://blast.jcvi.org/tgi_maize/index.cgi), high-throughput genomic sequences from bacterial artificial chromosome clones at the National Center for Biotechnology Information (NCBI; http://www.ncbi.nlm.nih.gov/HTGS), and the recent release of the maize genome sequence (http://maizesequence.org). The members of the maize *ASR* gene family suggested from these combined in silico analyses were confirmed by sequencing of amplified cDNA and genomic DNA of maize B73 plus one to five additional maize inbred lines (Mo17, F2, F252, MBS847, and/or A188). They were then mapped on the intermated B73 × Mo17 (IBM) or F2 × F252 (LHRF) mapping panels using the REFMAP050110 (IBM_Gnp2004) or LHRF_Gnp2004 framework map, respectively (Falque et al., 2005), using gene-specific primers (Supplemental Table S2). Alternatively, BLAST analysis on MaizeSequence.org was used in the absence of polymorphism between the maize inbred lines that led to the IBP or LHRF mapping panels. Deduced amino acid sequences were annotated by BLAST against known ASR proteins at NCBI and query against InterPro (http://www.ebi.ac.uk/Tools/pfa/iprscan/). The ProtParam tool (Gasteigler et al., 2005; http://web.expasy.org/protparam) was also used to determine the physical and chemical properties of the deduced amino acid sequences.

Phylogenetic Analysis

Sequence alignments were managed using BioEdit version 7.0.0 (Hall, 1999) and visually refined on the basis of the amino acid sequences. Bayesian phylogenetic analysis was carried out using MrBayes version 3.1.1 (Huelsenbeck and Ronquist, 2001) with a general time-reversible model, with a proportion of invariable sites and a γ-distribution for site-specific rates and a partition according to the three codon positions on the four most conserved regions only (272-nucleotide alignment matrix). Three chains (two-heated) were run twice for 10^7 generations, with a sampling of the cold chain parameters every 100 generations and a burn-in of 25,000 samples. Convergence was followed with potential scale reduction factor and average SD of split frequencies. A majority rule consensus tree was built with posterior probabilities of nodes above 0.85 × 100 indicated.

qRT-PCR and RT-PCR Analyses

The total RNA isolation from maize tissues collected in the stress experiments (leaves, roots, mature ovules, and kernels) with the TRIzol Reagent (Invitrogen) and ethanol precipitation was carried out as described (Trouverie et al., 2004). Subsequent DNase treatment and DNase inactivation were carried out according to the instructions of the supplier (Ambion). Two micrograms of total RNA was reverse transcribed using random hexamers (Invitrogen), 100 units of SuperScript II (Invitrogen), and 40 units of recombinant Rnasin RNase inhibitor (Promega) in a final volume of 20 μL. For expression profiles during maize ovule and kernel development, the total RNA isolation with phenol/chloroform extraction and acetic acid/ethanol precipitation, as well as subsequent DNase treatment and RT, were carried out as described (Massonneau et al., 2005).

Primer sequences were designed using Primer Express 2.0 (Applied Biosystem). Subsequent qRT-PCR analysis was carried out as described (Capelle et al., 2010). The calibration step of the experiment checked for equivalent PCR efficiency of the different genes (to allow comparison and normalization). Standard curves (log of cDNA dilution versus cycle threshold) using serial 10-fold dilution of cDNA were built for each pair of selected primers, a 100% efficiency corresponding to a slope of −3.3 (Marino et al., 2003). Practically, only pairs of primers yielding a slope of -3.3 ± 0.1 were selected. The specificity of the amplification (checked by dissociation curve analysis, gel electrophoresis, and sequencing of the PCR product) and the use of appropriate control genes were also assessed. Normalization of the results was achieved using the *Gly-rich RNA-binding protein2* (*ZmGRP2*) gene. After an initial test of five genes (*actin*, *polyubiquitin*, *α-tubulin*, *H^+-ATPase*, and *ZmGRP2*) on the range of tissues and treatments we wished to compare, only *ZmGRP2* was found to be stably expressed, in agreement with recent genome-wide observations in 55 tissues of maize B73 line (Sekhon et al., 2011). Conventional RT-PCR analysis was used to provide evidence that *ZmASR7-2* and *ZmASR7-3* genes are expressed. It was performed using the real-time PCR system and the SYBR Green PCR master mix as described (Capelle et al., 2010) to allow comparison with the qRT-PCR experiments. Products of the PCR were loaded on agarose gels and stained with ethidium bromide.

Microarray Analysis

Total RNA was extracted using the Nucleospin 8 RNA Extraction Kit (Macherey-Nagel) and in vitro amplified based on suggestions from the Maize Oligonucleotide Array Project (http://www.maizearray.org/files/cRNA_Target_Production_Using_RNA_Amplification.pdf). Hybridization was carried out as described (http://www.maizearray.org/files/Hybridization_Protocol_For_cRNA_Targets.pdf) using the 46K array constructed by the Maize Oligonucleotide Array Project. Quantile normalization of the raw data was carried out using the R version 2.4.1 software with a $\log_{10}$ transformation of the data initially performed. The criteria for the inclusion of a gene in the list of differentially expressed genes were a 1.5-fold increase or decrease and $P < 0.01$ by two-way ANOVA. The cDNA and genomic sequences corresponding to the 70-mers present on the microarray were established by BLAST of the 70-mers against the high-throughput genomic sequences database and the recent release of the maize genome sequence and regularly updated. Deduced amino acid sequences were annotated by BLAST against the Arabidopsis (*Arabidopsis thaliana*) genome at NCBI and screened for known conserved domains using the Center for Biological Sequence Analysis database (http://www.cbs.dtu.dk/services/).

Protein Extraction, Gel Staining, and 2-DE Analysis

Protein extraction with TCA/acetone precipitation was carried out as described (Méchin et al., 2007). Proteins were solubilized in UKS (for urea-K_2CO_3-sodium dodecyl sulfate) buffer (Méchin et al., 2007) and quantified using the 2-D Quant Kit (GE Healthcare Life Sciences). Isoelectrofocusing was carried out using 24-cm-long, pH 4 to 7 Immobiline Dry Strips (GE Healthcare Life Sciences) to which 50 μg (for protein quantification; 150 and 30 μg for ear leaf and kernel tissues, respectively) or 300 μg (for protein identification) of dissolved protein was added. Active rehydration and focusing were achieved

at 20°C in a Protean IEF Cell (Bio-Rad) by increasing the voltage step by step from 50 to 10,000 V (13 h at 50 V, 0.5 h at 200 V, 0.5 h at 500 V, 1 h at 1,000 V, then increase to 10,000 V) and stopped when 84,000 Vh was reached. Strips were equilibrated as described (Görg et al., 1987) and sealed at the top of a 1-mm-thick two-dimensional gel (24 × 22 cm) with 1% (w/v) low-melting agarose in SDS electrophoresis buffer (25 mM Trizma base, 0.2 M Gly, and 0.1% [v/v] SDS). Separation of continuous gels (11% [w/v] acrylamide, 2.9% [w/v] piperazine diacrylamide) was performed at 14°C (20 V for 1 h, 140 V for 15 h, and 20 V for 2 h) in a Protean Plus Dodeca Cell Electrophoresis Chamber (Bio-Rad) until the bromphenol blue front reached the end of the gel. For protein quantification, a silver-staining procedure was performed as described (Méchin et al., 2003). Scanning was carried out at 300 dpi with a 16-bit grayscale pixel depth using an image scanner (Amersham Biosciences) and analyzed with Progenesis software (Nonlinear Dynamics) according to Zivy (2007). For protein identification, gels were stained in colloidal Coomassie blue according to Yan et al. (2000) and spots were excised for MS. Excised gels were restained with silver nitrate as described (Méchin et al., 2003) and compared with the nonexcised silver-stained gels.

LC-MS/MS and Protein Identification

Two-dimensional gel spot digestion and LC-MS/MS analysis were performed as described (Page et al., 2010). A database search was performed with X!Tandem (version 2010.01.01.4; http://www.thegpm.org/tandem/). Enzymatic cleavage was declared as a trypsin digestion with one possible miscleavage. Cys carboxyamidomethylation and Met oxidation were set to static and possible modifications, respectively. Precursor mass and fragment mass tolerance were 2.0 and 0.8, respectively. A refinement search was added with similar parameters, except that semitryptic peptide and possible N-terminal protein acetylation were searched. The maize genome sequence (release 4a.53; 53,764 entries), the UniProt database restricted to maize (http://www.uniprot.org; release 15.11; 43,694 entries), and a contaminant database including in particular trypsin and keratins were used. Only peptides with a E value smaller than 0.1 were reported. Identified proteins were filtered and grouped using the X! Tandem pipeline (http://pappso.inra.fr/bioinfo/xtandempipeline/) with the following criteria: (1) a minimum of two different peptides was required with an E value smaller than 0.05; (2) a protein E value (calculated as the product of unique peptide E values) smaller than 10^{-4} was required. In the case of identification with only two or three MS/MS spectra, similarity between the experimental and the theoretical MS/MS spectra was visually checked. To take redundancy into account, proteins with at least one peptide in common were grouped. This allowed grouping of proteins of similar function. Within each group, proteins with at least one specific peptide relative to other members of the group were reported as subgroups.

Chlorophyll Content Measurement and Metabolite Analysis

Total chlorophyll content was measured after extraction of leaf material into 80% acetone and assay at 663 and 645 nm as described (Arnon, 1949). Gas chromatography coupled to time-of-flight MS analysis was carried out as described (Noctor et al., 2007). Because automated peak integration was occasionally erroneous, integration was verified manually for each compound in all analyses.

Two-Way ANOVA and Within-Group Correlation Matrix Analysis

A $\log_{10}$ transformation of the data was initially performed when the SE values showed that the SE increased in proportion to the treatment. Either nontransformed or $\log_{10}$-transformed values were then used for two-way ANOVA using R software version 2.8.1 (http://cran.at.r-project.org). The two possible means models for two-way ANOVA are the additive model and the interaction model (Scheffé, 1999; Seltman, 2010). An *F* test for interactions was performed to determine whether the additive model could be retained. When the interaction model was needed, the Bonferroni method was applied for pairwise comparisons. The significance was placed at the 0.05 level.

In a multivariate ANOVA model, the within-group correlation matrix is calculated from the correlation matrix of residuals after regressing out the influence of the fixed effects by linear regression (Hair et al., 2010). Functions of the R software were used. We were unable to test the association between two variables independently of the others because we did not have enough data to determine partial correlation coefficients. Therefore, the null hypothesis of a pairwise correlation coefficient was evaluated by a test derived from an *F* test and extended to all correlation coefficients using the Bonferroni method. The significance was placed at the 0.05 level.

Supplemental Data

The following materials are available in the online version of this article.

Supplemental Figure S1. Majority rule consensus tree obtained using Bayesian interference analysis of 100 *ASR* sequences.

Supplemental Figure S2. Stress treatment and yield trial of *ZmASR1*-OE plants.

Supplemental Figure S3. Relative expression profile of selected genes encoding ZmASR1 targets and/or rate-limiting enzymes in leaves 11 of *ZmASR1*-OE and wild-type plants.

Supplemental Figure S4. Transcript levels of *ZmASR7-1*, *ZmASR7-2*, and *ZmASR7-3* genes in leaf and root tissues.

Supplemental Table S1. *ZmASR* gene mapping.

Supplemental Table S2. Sequences of the primers used for mapping and qRT-PCR analyses.

Supplemental Table S3. Sequence identity between individual *ZmASR* genes.

Supplemental Table S4. Summary of exon lengths of various *ASR* genes from Poaceae and properties of their deduced amino acid sequences.

Supplemental Table S5. *ZmASR1*-OE plants maintain kernel yield under water-limited conditions.

Supplemental Table S6. Proteins that showed significant changes in *ZmASR1*-OE leaves compared with wild-type leaves, their annotated function, location, and quantification.

Supplemental Table S7. Unique metabolites identified in *ZmASR1*-OE and wild-type leaves.

Supplemental Table S8. Within-group correlation matrix.

Supplemental Table S9. Number of individual significant correlations for the whole matrix and its submatrices.

Supplemental Table S10. Pairwise correlations of ZmASR1 targets against BCAA-related ZmASR1 targets.

Supplemental Table S11. Pairwise correlations of ZmASR1 target transcripts against decreased and/or biomass-related metabolites.

ACKNOWLEDGMENTS

We thank Ingrid Doridant and Carine Hécart for maize transformation and culture, Carine Remoué for help with physical mapping, the Biogemma transcriptomic team for the hybridization and analysis of the microarray, and Jean Coursol for guiding us through the statistical analyses. Caroline Lelarge-Trouverie is acknowledged for preliminary metabolomic analysis on *ZmASR1*-OE.

Received March 22, 2011; accepted August 4, 2011; published August 18, 2011.

LITERATURE CITED

Amitai-Zeigerson H, Scolnik PA, Bar-Zvi D (1995) Tomato Asrl mRNA and protein are transiently expressed following salt stress, osmotic stress and treatment with abscisic acid. Plant Sci **110:** 205–213

Arnon DI (1949) Copper enzymes in isolated chloroplasts: polyphenoloxidase in *Beta vulgaris*. Plant Physiol **24:** 1–15

Battaglia M, Olvera-Carrillo Y, Garciarrubio A, Campos F, Covarrubias AA (2008) The enigmatic LEA proteins and other hydrophilins. Plant Physiol **148:** 6–24

Binder S, Knill T, Schuster J (2007) Branched-chain amino acid metabolism in higher plants. Physiol Plant **129:** 68–78

Böhmer M, Schroeder JI (2011) Quantitative transcriptomic analysis of

abscisic acid-induced and reactive oxygen species-dependent expression changes and proteomic profiling in Arabidopsis suspension cells. Plant J **67:** 105–118

Boyer JS, Westgate ME (2004) Grain yields with limited water. J Exp Bot **55:** 2385–2394

Brini F, Hanin M, Lumbreras V, Amara I, Khoudi H, Hassairi A, Pagès M, Masmoudi K (2007) Overexpression of wheat dehydrin DHN-5 enhances tolerance to salt and osmotic stress in *Arabidopsis thaliana*. Plant Cell Rep **26:** 2017–2026

Brini F, Saibi W, Amara I, Gargouri A, Masmoudi K, Hanin M (2010) Wheat dehydrin DHN-5 exerts a heat-protective effect on β-glucosidase and glucose oxidase activities. Biosci Biotechnol Biochem **74:** 1050–1054

Cakir B, Agasse A, Gaillard C, Saumonneau A, Delrot S, Atanassova R (2003) A grape ASR protein involved in sugar and abscisic acid signaling. Plant Cell **15:** 2165–2180

Cañas RA, Quilleré I, Lea PJ, Hirel B (2010) Analysis of amino acid metabolism in the ear of maize mutants deficient in two cytosolic glutamine synthetase isoenzymes highlights the importance of asparagine for nitrogen translocation within sink organs. Plant Biotechnol J **8:** 966–978

Canel C, Bailey-Serres JN, Roose ML (1995) Pummelo fruit transcript homologous to ripening-induced genes. Plant Physiol **108:** 1323–1324

Capelle V, Remoué C, Moreau L, Reyss A, Mahé A, Massonneau A, Falque M, Charcosset A, Thévenot C, Rogowsky P, et al (2010) QTLs and candidate genes for desiccation and abscisic acid content in maize kernels. BMC Plant Biol **10:** 2

Carrari F, Fernie AR, Iusem ND (2004) Heard it through the grapevine? ABA and sugar cross-talk: the ASR story. Trends Plant Sci **9:** 57–59

Castiglioni P, Warner D, Bensen RJ, Anstrom DC, Harrison J, Stoecker M, Abad M, Kumar G, Salvador S, D'Ordine R, et al (2008) Bacterial RNA chaperones confer abiotic stress tolerance in plants and improved grain yield in maize under water-limited conditions. Plant Physiol **147:** 446–455

Ciais P, Reichstein M, Viovy N, Granier A, Ogée J, Allard V, Aubinet M, Buchmann N, Bernhofer C, Carrara A, et al (2005) Europe-wide reduction in primary productivity caused by the heat and drought in 2003. Nature **437:** 529–533

Claassen HC (1970) The determination of low levels of cobalt-60 in environmental waters by liquid scintillation counting. Anal Chim Acta **52:** 229–235

Damerval C, Maurice A, Josse JM, de Vienne D (1994) Quantitative trait loci underlying gene product variation: a novel perspective for analyzing regulation of genome expression. Genetics **137:** 289–301

de Kraker JW, Luck K, Textor S, Tokuhisa JG, Gershenzon J (2007) Two Arabidopsis genes (*IPMS1* and *IPMS2*) encode isopropylmalate synthase, the branchpoint step in the biosynthesis of leucine. Plant Physiol **143:** 970–986

Depège-Fargeix N, Javelle M, Chambrier P, Frangne N, Gerentes D, Perez P, Rogowsky PM, Vernoud V (2011) Functional characterization of the HD-ZIP IV transcription factor OCL1 from maize. J Exp Bot **62:** 293–305

de Vienne D, Leonardi A, Damerval C, Zivy M (1999) Genetics of proteome variation for QTL characterization: application to drought-stress response in maize. J Exp Bot **50:** 303–309

Doczi R, Csanaki C, Banfalvi Z (2002) Expression and promoter activity of the desiccation-specific *Solanum tuberosum* gene, *StDS2*. Plant Cell Environ **25:** 1197–1203

Endler A, Meyer S, Schelbert S, Schneider T, Weschke W, Peters SW, Keller F, Baginsky S, Martinoia E, Schmidt UG (2006) Identification of a vacuolar sucrose transporter in barley and Arabidopsis mesophyll cells by a tonoplast proteomic approach. Plant Physiol **141:** 196–207

Falque M, Décousset L, Dervins D, Jacob AM, Joets J, Martinant JP, Raffoux X, Ribière N, Ridel C, Samson D, et al (2005) Linkage mapping of 1454 new maize candidate gene loci. Genetics **170:** 1957–1966

Fang LY, Gross PR, Chen CH, Lillis M (1992) Sequence of two acetohydroxyacid synthase genes from *Zea mays*. Plant Mol Biol **18:** 1185–1187

Food and Agriculture Organization of the United Nations (2008) Climate change, water and food security. http://www.fao.org/nr/water/docs/HLC08-FAOWater-E.pdf (February 26, 2008)

Frankel N, Nunes-Nesi A, Balbo I, Mazuch J, Centeno D, Iusem ND, Fernie AR, Carrari F (2007) *ci21A/Asr1* expression influences glucose accumulation in potato tubers. Plant Mol Biol **63:** 719–730

Friso G, Majeran W, Huang M, Sun Q, van Wijk KJ (2010) Reconstruction of metabolic pathways, protein expression, and homeostasis machineries across maize bundle sheath and mesophyll chloroplasts: large-scale quantitative proteomics using the first maize genome assembly. Plant Physiol **152:** 1219–1250

Furumoto T, Hata S, Izui K (2000) Isolation and characterization of cDNAs for differentially accumulated transcripts between mesophyll cells and bundle sheath strands of maize leaves. Plant Cell Physiol **41:** 1200–1209

Garay-Arroyo A, Colmenero-Flores JM, Garciarrubio A, Covarrubias AA (2000) Highly hydrophilic proteins in prokaryotes and eukaryotes are common during conditions of water deficit. J Biol Chem **275:** 5668–5674

Gasteigler E, Hoogland C, Gattiker A, Duvaud S, Wilkins MR, Appel RD, Bairoch A (2005) Protein identification and analysis tools on ExPASy server. *In* JM Walker, ed, The Proteomics Protocols Handbook. Humana Press, New York, pp 571–607

Goldgur Y, Rom S, Ghirlando R, Shkolnik D, Shadrin N, Konrad Z, Bar-Zvi D (2007) Desiccation and zinc binding induce transition of tomato abscisic acid stress ripening 1, a water stress- and salt stress-regulated plant-specific protein, from unfolded to folded state. Plant Physiol **143:** 617–628

Görg A, Postel W, Weser J, Günther S, Strahler JR, Hanash SM, Somerlot L (1987) Elimination of point streaking on silver stained two-dimensional gels by addition of iodoacetamide to the equilibration buffer. Electrophoresis **8:** 122–124

Guo AY, Zhu QH, Gu X, Ge S, Yang J, Luo J (2008) Genome-wide identification and evolutionary analysis of the plant specific SBP-box transcription factor family. Gene **418:** 1–8

Hair JF, Black WC, Babin BJ, Anderson RE (2010) Multivariate Data Analysis, Ed 7. Prentice Hall, Upper Saddle River, NJ

Hall TA (1999) BioEdit: a user-friendly biological sequence alignment editor and analysis program for Windows 95/98/NT. Nucl Acids Symp Ser **41:** 95–98

He Y, Mawhinney TP, Preuss ML, Schroeder AC, Chen B, Abraham L, Jez JM, Chen S (2009) A redox-active isopropylmalate dehydrogenase functions in the biosynthesis of glucosinolates and leucine in Arabidopsis. Plant J **60:** 679–690

Henry IM, Carpentier SC, Pampurova S, Van Hoylandt A, Panis B, Swennen R, Remy S (June 1, 2011) Structure and regulation of the *Asr* gene family in banana. Planta http://dx.doi.org/10.1007/s00425-011-1421-0

Huang JC, Lin SM, Wang CS (2000) A pollen-specific and desiccation-associated transcript in *Lilium longiflorum* during development and stress. Plant Cell Physiol **41:** 477–485

Huelsenbeck JP, Ronquist F (2001) MRBAYES: Bayesian inference of phylogenetic trees. Bioinformatics **17:** 754–755

Ishida Y, Saito H, Ohta S, Hiei Y, Komari T, Kumashiro T (1996) High efficiency transformation of maize (*Zea mays* L.) mediated by *Agrobacterium tumefaciens*. Nat Biotechnol **14:** 745–750

Iusem ND, Bartholomew DM, Hitz WD, Scolnik PA (1993) Tomato (*Lycopersicon esculentum*) transcript induced by water deficit and ripening. Plant Physiol **102:** 1353–1354

Jeanneau M, Gerentes D, Foueillassar X, Zivy M, Vidal J, Toppan A, Perez P (2002) Improvement of drought tolerance in maize: towards the functional validation of the *Zm-Asr1* gene and increase of water use efficiency by over-expressing C4-PEPC. Biochimie **84:** 1127–1135

Joshi V, Joung JG, Fei Z, Jander G (2010) Interdependence of threonine, methionine and isoleucine metabolism in plants: accumulation and transcriptional regulation under abiotic stress. Amino Acids **39:** 933–947

Kalifa Y, Gilad A, Konrad Z, Zaccai M, Scolnik PA, Bar-Zvi D (2004a) The water- and salt-stress-regulated *Asr1* (abscisic acid stress ripening) gene encodes a zinc-dependent DNA-binding protein. Biochem J **381:** 373–378

Kalifa Y, Perlson A, Gilad A, Konrad Z, Scolnik PA, Bar-Zvi D (2004b) Over-expression of the water and salt stress-regulated *Asr1* gene confers an increased salt tolerance. Plant Cell Environ **27:** 1459–1468

Kerk D, Bulgrien J, Smith DW, Gribskov M (2003) Arabidopsis proteins containing similarity to the universal stress protein domain of bacteria. Plant Physiol **131:** 1209–1219

Koch KE (1996) Carbohydrate-modulated gene expression in plants. Annu Rev Plant Physiol Plant Mol Biol **47:** 509–540

Komari T, Hiei Y, Saito Y, Murai N, Kumashiro T (1996) Vectors carrying two separate T-DNAs for co-transformation of higher plants mediated by Agrobacterium tumefaciens and segregation of transformants free from selection markers. Plant J **10:** 165–174

Konrad Z, Bar-Zvi D (2008) Synergism between the chaperone-like activity

of the stress regulated ASR1 protein and the osmolyte glycine-betaine. Planta **227:** 1213–1219

Less H, Angelovici R, Tzin V, Galili G (2010) Principal transcriptional regulation and genome-wide system interactions of the Asp-family and aromatic amino acid networks of amino acid metabolism in plants. Amino Acids **39:** 1023–1028

Less H, Galili G (2008) Principal transcriptional programs regulating plant amino acid metabolism in response to abiotic stresses. Plant Physiol **147:** 316–330

Li P, Ponnala L, Gandotra N, Wang L, Si Y, Tausta SL, Kebrom TH, Provart N, Patel R, Myers CR, et al (2010) The developmental dynamics of the maize leaf transcriptome. Nat Genet **42:** 1060–1067

Liu HY, Dai JR, Feng DR, Liu B, Wang HB, Wang JF (2010) Characterization of a novel plantain *Asr* gene, *MpAsr,* that is regulated in response to infection of *Fusarium oxysporum* f. sp. *cubense* and abiotic stresses. J Integr Plant Biol **52:** 315–323

Lu G-H, Tang J-H, Yan F-B, Ma X-Q, Li J-S, Chen S-J, Ma J-C, Liu Z-X, E L-Z, Zhang Y-R, et al (2006) Quantitative trait loci mapping of maize yield and its components under different water treatments at flowering time. J Integr Plant Biol **48:** 1233–1243

Majeran W, Cai Y, Sun Q, van Wijk KJ (2005) Functional differentiation of bundle sheath and mesophyll maize chloroplasts determined by comparative proteomics. Plant Cell **17:** 3111–3140

Majeran W, Friso G, Ponnala L, Connolly B, Huang M, Reidel EJ, Zhang C, Asakura Y, Bhuiyan NH, Sun Q, et al (2010) Structural and metabolic transitions of C_4 leaf development and differentiation defined by microscopy and quantitative proteomics in maize. Plant Cell **22:** 3509–3542

Marino JH, Cook P, Miller KS (2003) Accurate and statistically verified quantification of relative mRNA abundances using SYBR Green I and real-time RT-PCR. J Immunol Methods **283:** 291–306

Marino R, Ponnaiah M, Krajewski P, Frova C, Gianfranceschi L, Pè ME, Sari-Gorla M (2009) Addressing drought tolerance in maize by transcriptional profiling and mapping. Mol Genet Genomics **281:** 163–179

Martin A, Lee J, Kichey T, Gerentes D, Zivy M, Tatout C, Dubois F, Balliau T, Valot B, Davanture M, et al (2006) Two cytosolic glutamine synthetase isoforms of maize are specifically involved in the control of grain production. Plant Cell **18:** 3252–3274

Maskin L, Frankel N, Gudesblat G, Demergasso MJ, Pietrasanta LI, Iusem ND (2007) Dimerization and DNA-binding of ASR1, a small hydrophilic protein abundant in plant tissues suffering from water loss. Biochem Biophys Res Commun **352:** 831–835

Maskin L, Gudesblat G, Moreno J, Carrari F, Frankel N, Sambade A, Rossi M, Iusem ND (2001) Differential expression of the members of the *Asr* gene family in tomato (*Lycopersicon esculentum*). Plant Sci **161:** 739–746

Massonneau A, Condamine P, Wisniewski JP, Zivy M, Rogowsky PM (2005) Maize cystatins respond to developmental cues, cold stress and drought. Biochim Biophys Acta **1729:** 186–199

McPherson HG, Boyer J (1977) Regulation of grain yield by photosynthesis in maize subjected to water deficiency. Agron J **69:** 714–718

Méchin V, Consoli L, Le Guilloux M, Damerval C (2003) An efficient solubilization buffer for plant proteins focused in immobilized pH gradients. Proteomics **3:** 1299–1302

Méchin V, Damerval C, Zivy M (2007) Total protein extraction with TCA-acetone. Methods Mol Biol **355:** 1–8

Meyer RC, Steinfath M, Lisec J, Becher M, Witucka-Wall H, Törjék O, Fiehn O, Eckardt A, Willmitzer L, Selbig J, et al (2007) The metabolic signature related to high plant growth rate in *Arabidopsis thaliana*. Proc Natl Acad Sci USA **104:** 4759–4764

Montrichard F, Alkhalfioui F, Yano H, Vensel WH, Hurkman WJ, Buchanan BB (2009) Thioredoxin targets in plants: the first 30 years. J Proteomics **72:** 452–474

Murat F, Xu JH, Tannier E, Abrouk M, Guilhot N, Pont C, Messing J, Salse J (2010) Ancestral grass karyotype reconstruction unravels new mechanisms of genome shuffling as a source of plant evolution. Genome Res **20:** 1545–1557

Nakashima K, Ito Y, Yamaguchi-Shinozaki K (2009) Transcriptional regulatory networks in response to abiotic stresses in Arabidopsis and grasses. Plant Physiol **149:** 88–95

Nelson DE, Repetti PP, Adams TR, Creelman RA, Wu J, Warner DC, Anstrom DC, Bensen RJ, Castiglioni PP, Donnarummo MG, et al (2007) Plant nuclear factor Y (NF-Y) B subunits confer drought tolerance and lead to improved corn yields on water-limited acres. Proc Natl Acad Sci USA **104:** 16450–16455

Nishizawa A, Yabuta Y, Shigeoka S (2008) Galactinol and raffinose constitute a novel function to protect plants from oxidative damage. Plant Physiol **147:** 1251–1263

Noctor G, Bergot G, Thominet D, Mauve C, Lelarge-Trouverie C, Prioul JL (2007) A comparative study of amino acid analysis in leaf extracts by gas chromatography-time of flight-mass spectrometry and high performance liquid chromatography with fluorescence detection. Metabolomics **3:** 161–174

Padmanabhan V, Dias DM, Newton RJ (1997) Expression analysis of a gene family in loblolly pine (*Pinus taeda* L.) induced by water deficit stress. Plant Mol Biol **35:** 801–807

Page D, Gouble B, Valot B, Bouchet JP, Callot C, Kretzschmar A, Causse M, Renard CM, Faurobert M (2010) Protective proteins are differentially expressed in tomato genotypes differing for their tolerance to low-temperature storage. Planta **232:** 483–500

Pelleschi S, Leonardi A, Rocher J-P, Cornic G, de Vienne D, Thevenot C, Prioul JL (2006) Analysis of the relationships between growth, photosynthesis and carbohydrate metabolism using quantitative trait loci (QTLs) in young maize plants subjected to water deprivation. Mol Breed **17:** 21–39

Philippe R, Courtois B, McNally KL, Mournet P, El-Malki R, Le Paslier MC, Fabre D, Billot C, Brunel D, Glaszmann JC, et al (2010) Structure, allelic diversity and selection of *Asr* genes, candidate for drought tolerance, in *Oryza sativa* L. and wild relatives. Theor Appl Genet **121:** 769–787

Qin L, Trouverie J, Chateau-Joubert S, Simond-Côte E, Thevenot C, Prioul JL (2004) Involvement of the Ivr2-invertase in the perianth during maize kernel development under water stress. Plant Sci **166:** 371–379

Quan R, Shang M, Zhang H, Zhao Y, Zhang J (2004) Engineering of enhanced glycine betaine synthesis improves drought tolerance in maize. Plant Biotechnol J **2:** 477–486

Rabbani MA, Maruyama K, Abe H, Khan MA, Katsura K, Ito Y, Yoshiwara K, Seki M, Shinozaki K, Yamaguchi-Shinozaki K (2003) Monitoring expression profiles of rice genes under cold, drought, and high-salinity stresses and abscisic acid application using cDNA microarray and RNA gel-blot analyses. Plant Physiol **133:** 1755–1767

Riccardi F, Gazeau P, de Vienne D, Zivy M (1998) Protein changes in response to progressive water deficit in maize: quantitative variation and polypeptide identification. Plant Physiol **117:** 1253–1263

Riccardi F, Gazeau P, Jacquemot MP, Vincent D, Zivy M (2004) Deciphering genetic variations of proteome responses to water deficit in maize leaves. Plant Physiol Biochem **42:** 1003–1011

Rolland F, Baena-Gonzalez E, Sheen J (2006) Sugar sensing and signaling in plants: conserved and novel mechanisms. Annu Rev Plant Biol **57:** 675–709

Rom S, Gilad A, Kalifa Y, Konrad Z, Karpasas MM, Goldgur Y, Bar-Zvi D (2006) Mapping the DNA- and zinc-binding domains of ASR1 (abscisic acid stress ripening), an abiotic-stress regulated plant specific protein. Biochimie **88:** 621–628

Rossi M, Carrari F, Cabrera-Ponce JL, Vázquez-Rovere C, Herrera-Estrella L, Gudesblat G, Iusem ND (1998) Analysis of an abscisic acid (ABA)-responsive gene promoter belonging to the *Asr* gene family from tomato in homologous and heterologous systems. Mol Gen Genet **258:** 1–8

Salekdeh GH, Reynolds M, Bennett J, Boyer J (2009) Conceptual framework for drought phenotyping during molecular breeding. Trends Plant Sci **14:** 488–496

Salse J, Bolot S, Throude M, Jouffe V, Piegu B, Quraishi UM, Calcagno T, Cooke R, Delseny M, Feuillet C (2008) Identification and characterization of shared duplications between rice and wheat provide new insight into grass genome evolution. Plant Cell **20:** 11–24

Saumonneau A, Agasse A, Bidoyen MT, Lallemand M, Cantereau A, Medici A, Laloi M, Atanassova R (2008) Interaction of grape ASR proteins with a DREB transcription factor in the nucleus. FEBS Lett **582:** 3281–3287

Scheffé H (1999) The Analysis of Variance. John Wiley & Sons, New York

Schnable PS, Ware D, Fulton RS, Stein JC, Wei F, Pasternak S, Liang C, Zhang J, Fulton L, Graves TA, et al (2009) The B73 maize genome: complexity, diversity, and dynamics. Science **326:** 1112–1115

Schneider A, Salamini F, Gebhardt C (1997) Expression patterns and promoter activity of the cold-regulated gene *ci21A* of potato. Plant Physiol **113:** 335–345

Sekhon RS, Lin H, Childs KL, Hansey CN, Buell CR, de Leon N,

Kaeppler SM (2011) Genome-wide atlas of transcription during maize development. Plant J **66:** 553–563

Seltman HJ (2010) Experimental design and analysis. http://www.stat.cmu.edu/~hseltman/309/Book/Book.pdf (September 8, 2011)

Shkolnik D, Bar-Zvi D (2008) Tomato ASR1 abrogates the response to abscisic acid and glucose in Arabidopsis by competing with ABI4 for DNA binding. Plant Biotechnol J **6:** 368–378

Silhavy D, Hutvágner G, Barta E, Bánfalvi Z (1995) Isolation and characterization of a water-stress-inducible cDNA clone from *Solanum chacoense*. Plant Mol Biol **27:** 587–595

Stone JM, Liang X, Nekl ER, Stiers JJ (2005) Arabidopsis AtSPL14, a plant-specific SBP-domain transcription factor, participates in plant development and sensitivity to fumonisin B1. Plant J **41:** 744–754

Sugiharto B, Ermawati N, Mori H, Aoki K, Yonekura-Sakakibara K, Yamaya T, Sugiyama T, Sakakibara H (2002) Identification and characterization of a gene encoding drought-inducible protein localizing in the bundle sheath cell of sugarcane. Plant Cell Physiol **43:** 350–354

Sulpice R, Pyl ET, Ishihara H, Trenkamp S, Steinfath M, Witucka-Wall H, Gibon Y, Usadel B, Poree F, Piques MC, et al (2009) Starch as a major integrator in the regulation of plant growth. Proc Natl Acad Sci USA **106:** 10348–10353

Szabados L, Savouré A (2010) Proline: a multifunctional amino acid. Trends Plant Sci **15:** 89–97

Taji T, Ohsumi C, Iuchi S, Seki M, Kasuga M, Kobayashi M, Yamaguchi-Shinozaki K, Shinozaki K (2002) Important roles of drought- and cold-inducible genes for galactinol synthase in stress tolerance in *Arabidopsis thaliana*. Plant J **29:** 417–426

Takasaki H, Mahmood T, Matsuoka M, Matsumoto H, Komatsu S (2008) Identification and characterization of a gibberellin-regulated protein, which is ASR5, in the basal region of rice leaf sheaths. Mol Genet Genomics **279:** 359–370

Tardieu F, Reymond M, Hamard P, Granier C, Muller B (2000) Spatial distributions of expansion rate, cell division rate and cell size in maize leaves: a synthesis of the effects of soil water status, evaporative demand and temperature. J Exp Bot **51:** 1505–1514

Trouverie J, Chateau-Joubert S, Thévenot C, Jacquemot MP, Prioul JL (2004) Regulation of vacuolar invertase by abscisic acid or glucose in leaves and roots from maize plantlets. Planta **219:** 894–905

Tuberosa R, Salvi S (2006) Genomics-based approaches to improve drought tolerance of crops. Trends Plant Sci **11:** 405–412

Udomprasert N, Kijjanon J, Thiraporn R, Machuay A (1999) Effects of water deficit at tasseling on proline and abscisic acid levels and yield of corn. Kasetsart J Nat Sci **33:** 310–316

Urano K, Maruyama K, Ogata Y, Morishita Y, Takeda M, Sakurai N, Suzuki H, Saito K, Shibata D, Kobayashi M, et al (2009) Characterization of the ABA-regulated global responses to dehydration in Arabidopsis by metabolomics. Plant J **57:** 1065–1078

Urtasun N, Correa García S, Iusem ND, Bermúdez Moretti M (2010) Predominantly cytoplasmic localization in yeast of ASR1, a non-receptor transcription factor from plants. Open Biochem J **4:** 68–71

Vaidyanathan R, Kuruvilla S, Thomas G (1999) Characterization and expression pattern of an abscisic acid and osmotic stress responsive gene from rice. Plant Sci **140:** 21–30

Verdaguer N, Sevilla N, Valero ML, Stuart D, Brocchi E, Andreu D, Giralt E, Domingo E, Mateu MG, Fita I (1998) A similar pattern of interaction for different antibodies with a major antigenic site of foot-and-mouth disease virus: implications for intratypic antigenic variation. J Virol **72:** 739–748

Wang CS, Liau YE, Huang JC, Wu TD, Su CC, Lin CH (1998) Characterization of a desiccation-related protein in lily pollen during development and stress. Plant Cell Physiol **39:** 1307–1314

Wang HJ, Hsu CM, Jauh GY, Wang CS (2005) A lily pollen ASR protein localizes to both cytoplasm and nuclei requiring a nuclear localization signal. Physiol Plant **123:** 314–320

Westgate ME, Steudle E (1985) Water transport in the midrib tissue of maize leaves: direct measurement of the propagation of changes in cell turgor across a plant tissue. Plant Physiol **78:** 183–191

Yan JX, Wait R, Berkelman T, Harry RA, Westbrook JA, Wheeler CH, Dunn MJ (2000) A modified silver staining protocol for visualization of proteins compatible with matrix-assisted laser desorption/ionization and electrospray ionization-mass spectrometry. Electrophoresis **21:** 3666–3672

Yang CY, Chen YC, Jauh GY, Wang CS (2005) A lily ASR protein involves abscisic acid signaling and confers drought and salt resistance in Arabidopsis. Plant Physiol **139:** 836–846

Yang CY, Wu CH, Jauh GY, Huang JC, Lin CC, Wang CS (2008) The LLA23 protein translocates into nuclei shortly before desiccation in developing pollen grains and regulates gene expression in Arabidopsis. Protoplasma **233:** 241–254

Zivy M (2007) Quantitative analysis of 2D gels. Methods Mol Biol **355:** 175–194

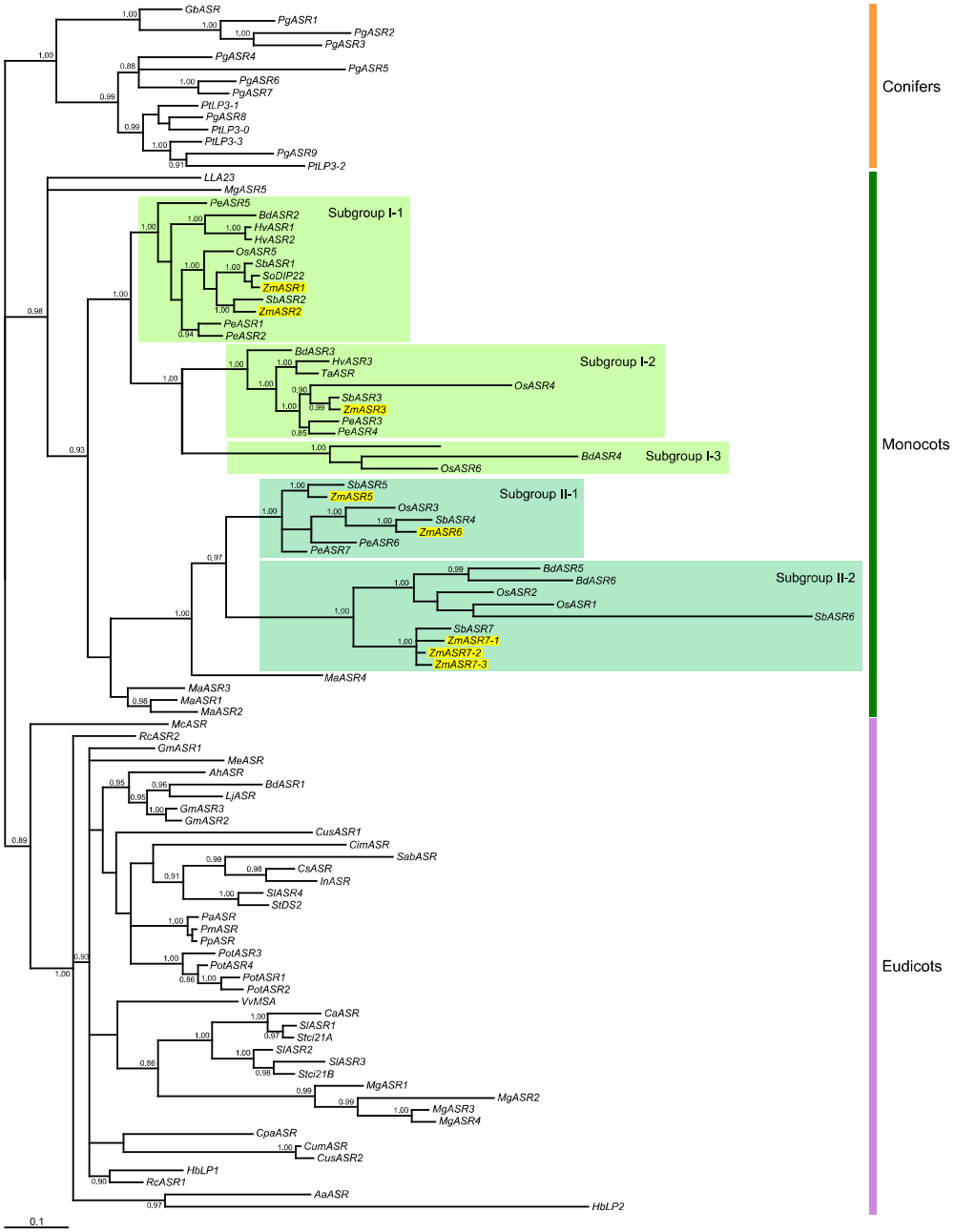

Figure S1. Majority rule consensus tree obtained using Bayesian inference analysis of 100 *ASR* sequences. Analysis was performed on a 272-nucleotide matrix restricted to 4 conserved regions (posterior probabilities of nodes above 0.8 indicated; tree rooted with the conifer group). Poaceae sequences fell in two distinct clades, the I-1/I-2/I-3 clade and the II-1/II-2 clade indicated in green and blue, respectively. Maize *ASR* genes are highlighted by yellow shading. Their accession numbers are indicated in Supplemental Table S1. Other accession numbers are as follows: for *Artemisia annua*, *AaASR* (EZ25607.1); for peanut, *AhASR* (EZ721040.1); for *Brachypodium distachyon*, *BdASR1* (Bradi5g10030.1), *BdASR2* (Bradi4g24650.1), *BdASR3* (Bradi5g10027.1), *BdASR4* (Bradi2g61590.1), *BdASR5* (Bradi2g61600.1), and *BdASR6* (Bradi2g61607.1); for cayenne pepper, *CaASR* (AY496130.1) ; for pomelo, *CimASR* (U18972.1) ; for papaya, *CpaASR* (TU.supercontig_21.214) ; for *Calystegia soldanella*, *CsASR* (AB047594) ; for muskmelon, *CumASR* (AF426403.1) ; for cucumber, *CusASR1* (Cucsa.325760.1), and *CuSASR2* (Cucsa.325770.1) ; for *Ginkgo biloba*, *GbASR* (AY461715.1); for soybean, *GmASR1* (AK285221.1), *GmASR2* (AK382827.1), and *GmASR3* (Glyma10g36890.1); for rubber tree, *HbLP1* (AY221984.1), and *HbLP2* (AY221987.1); for barley, *HvASR1* (AK252686.1), *HvASR2* (AK252200.1), and *HvASR3* (AK250239.1); for *Ipomea nil*, *InASR* (AB267819); for lotus, *LjASR* (AP004525); for lily, *LLA23* (AY101194.2); for banana, *MaASR1* (GU134749.1), *MaASR2* (GU134773.1), *MaASR3* (GU134777.1), and *MaASR4* (GU134737.1); for *Mesembryanthemum crystallinum*, *McASR* (AF054443); for cassava, *MeASR* (cassava19036); for *Mimulus gusttatus*, *MgASR1* (mgf006859m), *MgASR2* (mgf007644m), *MgASR3* (mgf010714m), *MgASR4* (mgf021948m), and *MgASR5* (mgf016130m); for rice, *OsASR1* (AK063053.1), *OsASR2* (AK318549.1), *OsASR3* (AK064115.1), *OsASR4* (AK104594.1), *OsASR5* (AK119208.1), and *OsASR6* (AK060804.1); for apricot, *PaASR (U93164.1);* for bamboo moso, *PeASR1* (FP096381.1), *PeASR2* (FP097460.1), *PeASR3* (FP096151.1), *PeASR4* (FP092024.1), *PeASR5* (FP097457.1), *PeASR6* (FP097681.1), and *PeASR7* (FP093510.1); for japanese apricot, *PmASR* (AB434493.1); for white spruce, *PgASR1* (BT114797), *PgASR2* (BT102053.1), *PgASR3* (BT106573.1), *PgASR4* (BT101799.1), *PgASR5* (BT101584.1), *PgASR6* (BT087197.1), *PgASR7* (BT102413.1), *PgASR8* (BT101475.1), and *PgASR9* (BT117663.1); for poplar, *PotASR1* (XM_002306668.1), *PotASR2* (XM_002306669.1), *PotASR3* (XM_002306670.1), and *PotASR4* (POPTR_0005s21570.1); for peach, *PpASR* (AF317062) ; for loblolly pine, *PtLP3-0* (U67135), *PtLP3-1* (U52865), *PtLP3-2* (U59451), and *PtLP3-3* (U59424) ; for castor oil plant, *RcASR1* (XM_002524251.1), and *RcASR2* (XM_002524250.1); for *Salicornia brachiata*, *SabASR* (EU746399.1); for sorghum, *SbASR1* (Sb08g004190.1), *SbASR2* (Sb05g004100.1), *SbASR3* (Sb06g016540.1), *SbASR4* (Sb04g022220.1), *SbASR5* (Sb06g016530.1), *SbASR6* (Sb03g013810.1), and *SbASR7* (Sb03g013820.1); for tomato, *SlASR1* (DQ058745.1), *SlASR2* (AY217012.1), *SlASR3* (DQ058750.1), and *SlASR4* (DQ058762.1); for sugarcane, *SoDIP22* (AB071694.1); for potato, *Stci21A* (U76610.1), *Stci21B* (U76611.1), and *StDS2* (AJ320154); for *Triticum aestivum*, *TaASR* (AK333819.1); for grapevine, *VvMSA* (AF281656.1).

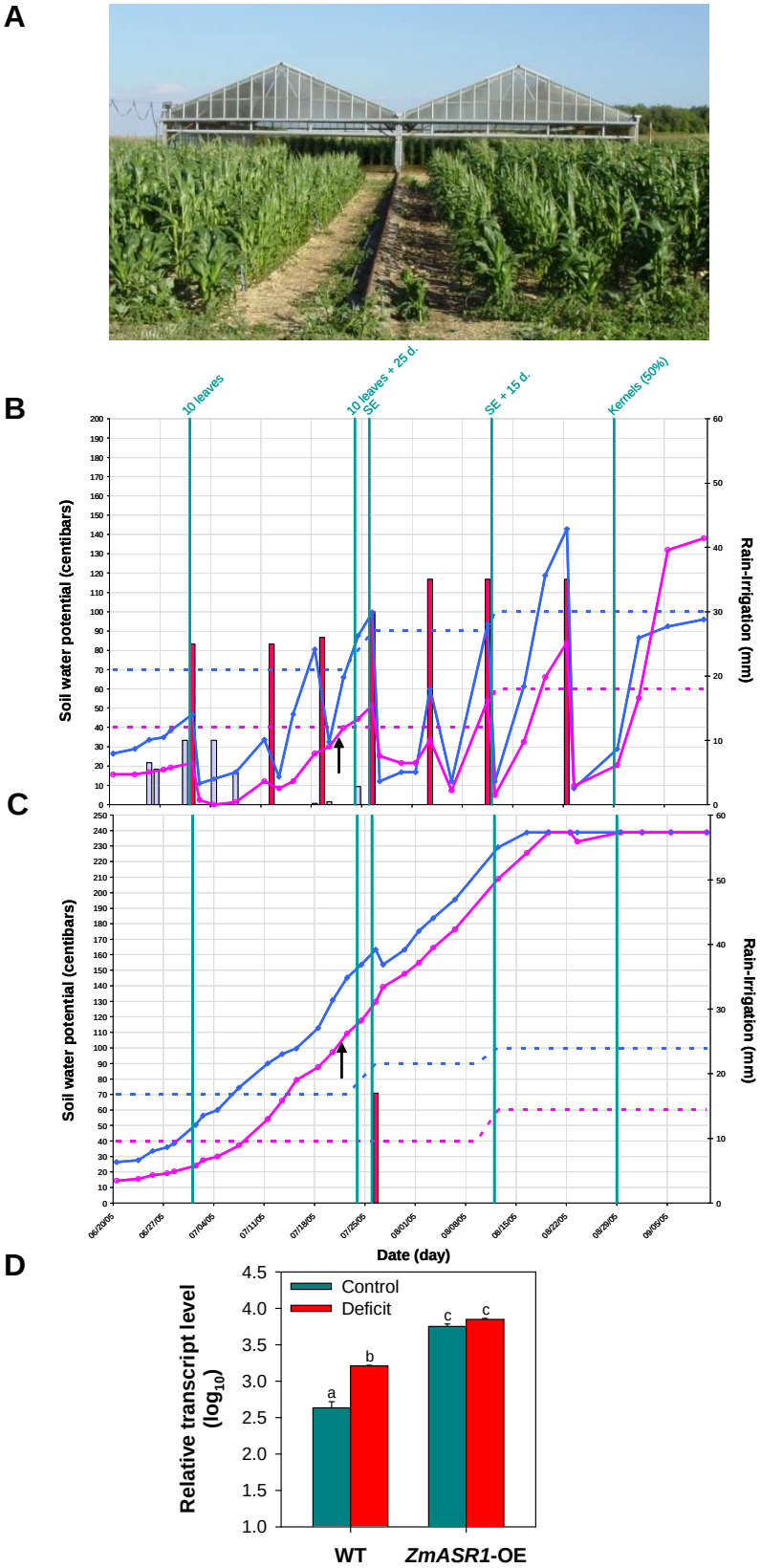

Figure S2. Stress treatment and yield trial of *ZmASR1*-OE plants. (A-C) The yield performance of 9 independently integrated T2 events was evaluated in the field at Magneraud, France, in May 2005, using two randomized block design. One block was maintained in a well-watered (control) condition (B) using rain and overhead irrigation, and the other one placed under limited water-supply (C) with mobile devices (A) preventing watering by rain (experimental details are described in Methods). Blue bar: rain; red bar: overhead irrigation; dashed blue line: threshold of depth (probe at 60 cm below the surface); dashed pink line: threshold of surface (probe at 30 cm below the surface); blue line: median of depth; pink line: median of surface; black arrow: harvest of leaves 11. (D) Quantitative RT-PCR experiments assessing *ZmASR1* relative expression in WT and *ZmASR1*-OE leaf samples at a developmental stage corresponding to 57 d after sowing (5 d before silk emergence) using gene-specific primers listed in Supplemental Table S2. Transcript levels were normalized against the stable endogenous *ZmGRP2* gene and shown relative to *ZmBCAT2* transcript levels in the 11th leaf in control conditions. Values represent the mean of biological duplicates ± SE. When two samples show different letters above the bar, the difference between them is significant (normal letters: $P < 0.05$).

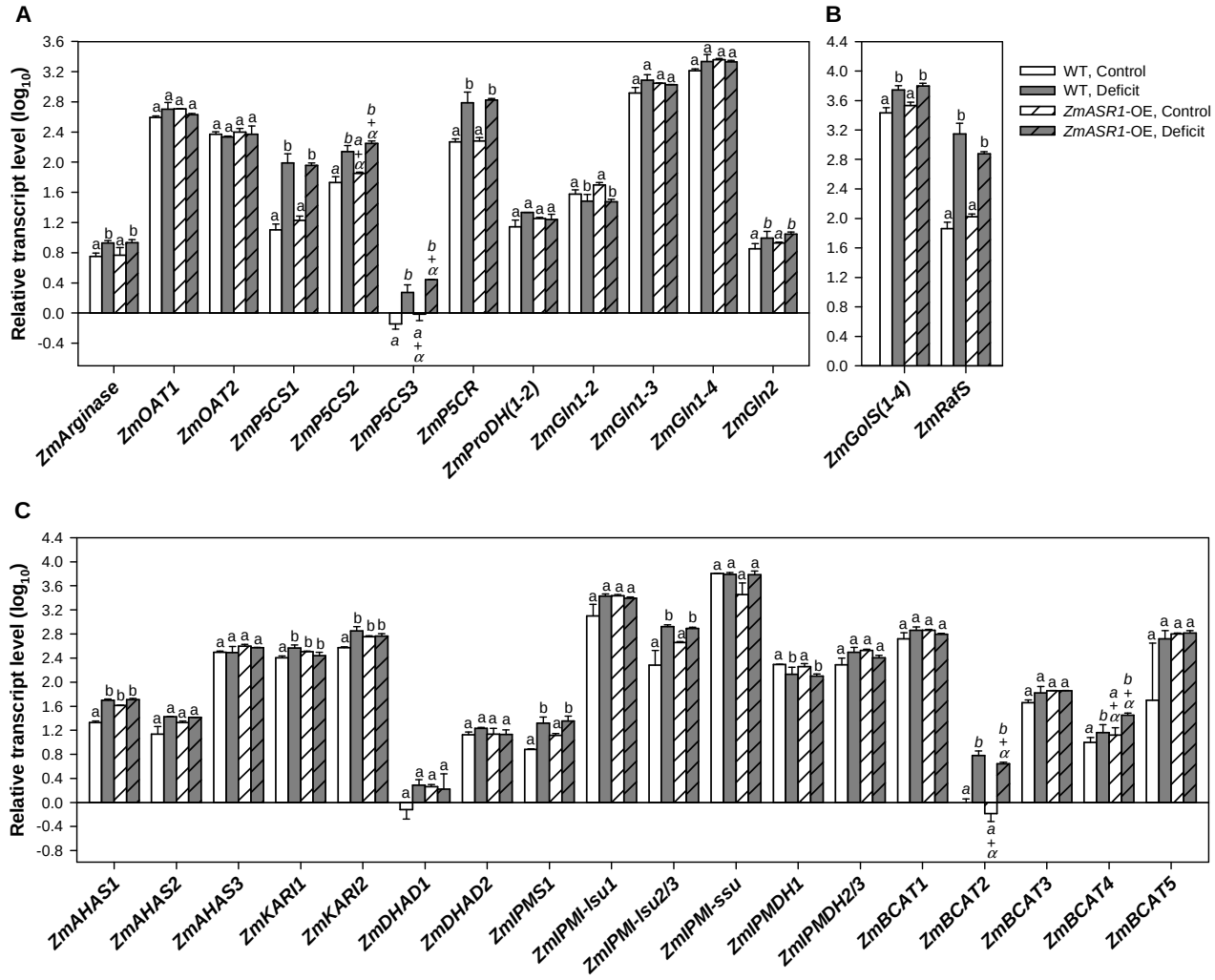

Figure S3. Relative expression profile of selected genes encoding ZmASR1 targets and/or rate-limiting enzymes in leaves 11 of *ZmASR1*-OE and WT plants. Glu (A), RFO (B) and BCAA (C) metabolisms. Quantitative RT-PCR experiments were carried out on cDNA prepared from WT and *ZmASR1*-OE leaf samples (pool of 3 events, 14 to 18 plants per event, 46 plants in total per sample) at a developmental stage corresponding to 57 d after sowing using gene-specific primers listed in Supplemental Table S2. Transcript levels were normalized with the values obtained for the *ZmGRP2* gene, which was used as an internal reference gene, and shown relative to *ZmBCAT2* transcript levels in leaf 11 in well-watered (control) conditions. Values represent the mean of biological duplicates ± SE (normal letters: $P < 0.05$; italic letters: $P < 0.10$). When both genotypes and treatment effects are significant, a, b, a+α and b+α are indicated (see the Methods section). AHAS, acetohydroxyacid synthase; BCAT, branched-chain aminotransferase; DHAD: dihydroxyacid dehydratase; Gln1, cytosolic Gln synthetase; Gln2, plastidic Gln synthetase; GolS, galactinol synthase; IPMDH, isopropylmalate dehydrogenase; IPMI-lsu: isopropylmalate isomerase large subunit; IPMI-ssu: isopropylmalate isomerase small subunit; IPMS: isopropylmalate synthase; KARI, Ketolacid reductoisomerase; OAT, ornithine-δ-aminotransferase; P5CS, Δ^1-pyrroline-5-carboxylate (P5C) synthetase 1; P5CR, P5C reductase; ProDH, Pro dehydrogenase; RafS, raffinose synthase.

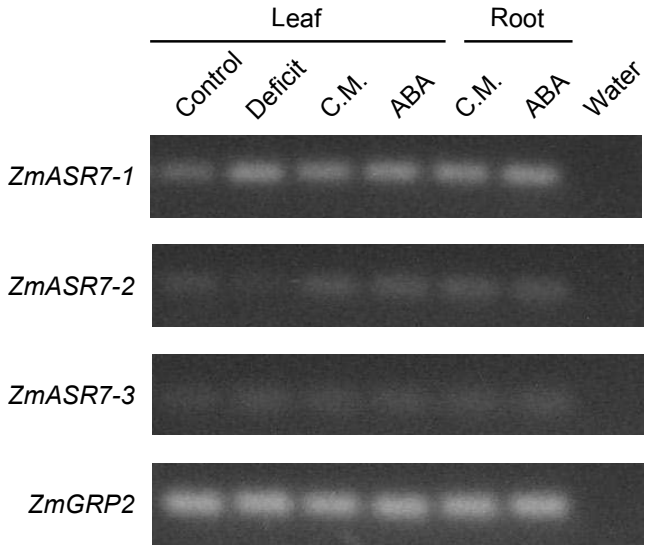

Figure S4. Transcript levels of *ZmASR7-1* , *ZmASR7-2* and *ZmASR7-3* genes in leaf and root tissues. RT-PCR was performed on total RNA of the indicated tissues using gene-specific primers (Supplemental Table S2), the 7500HT real-time PCR system and the SYBR green PCR master mix (Applied Biosystems) to allow comparison with the qRT-PCR experiments. The stable endogenous *ZmGRP2* gene was used as an internal control of RNA quantity. Water was used as a negative control of the PCR reaction. Products of the PCR reaction were then loaded on agarose gels and stained with ethidium bromide. The figure shows data representative of one of three separate experiments. Leaf: mature leaves of B73 plants grown under well-watered (control) or water deficit (deficit) conditions, and 10 d-old F2 plantlets supplied in continuous light during 12 h with culture medium (C.M.) or 3.7 µM ABA. Root: roots of 10 d-old F2 plantlets supplied in continuous light during 12 h with culture medium (C.M.) or 3.7 µM ABA.

Table S1. *ZmASR* gene mapping.

Gene name	Maize gene model[a]	Map[b]	Bin	MM coord.[c]	Proj. coord.[d]	Flanking Markers[e]
ZmASR1	GRMZM2G136910	REFMAP050110	10.02-10.03	49.6	143.5	phi059-umc130
ZmASR2	GRMZM5G854138	Physical	2.05	354.5	354.5	csu850-csu850
ZmASR3	GRMZM2G044132	LHRF_Gnp2004	2.04	197.1	314.9	bnlg1175-umc255a
ZmASR4	GRMZM2G168552	LHRF_Gnp2004	8.05	201	404.2	umc1665-bnlg1782
ZmASR5	GRMZM2G052100	REFMAP050110	10.04-10.05	92	294.4	bnlg1526-umc259
ZmASR6	GRMZM2G057841	REFMAP050110	5.04-5.05	215.9	388.7	bnl5.71a-phi333597
ZmASR7-1	GRMZM2G014797	Physical	3.04	238.1	238.1	AY110403-AY110403
ZmASR7-2	GRMZM2G314075	Physical	3.04	238.1	238.1	AY110403-AY110403
ZmASR7-3	GRMZM2G383699	Physical	3.04	238.1	238.1	AY110403-AY110403

[a]Maize genome release 5.a.59 of November 2010 (http://www.maizesequence.org).
[b]Mapping was performed on the IBM population (REFMAP050110 map) derived from B73xMo17 crossing, except for *ZmASR3* and *ZmASR4* genes, which were mapped on the LHRF_Gnp2004 population derived from F2xF252 crossing because of no polymorphism between B73 and Mo17, and *ZmASR7-1*, *ZmASR7-2* and *ZmASR7-3* genes, which were mapped by BLAST analysis on MaizeSequence.org because of no polymorphism between either B73 and Mo17, or F2 and F252.
[c]Map coordinate computed with MapMaker using "RI self Haldane" options or found on the HTGS database.
[d]Map coordinate on IBM2 2008 Neighbors obtained by homothetic projection with BioMercator (Arcade et al. 2004).
[e]Proximal and distal markers.

Table S2. Sequence of the primers used for mapping and qRT-PCR analyses.

Gene name and/or oligo ID[a]	Maize gene model[b]	Annotation[c]	Class	Used for	Primer name	Amplicon size (bp)	Sequence (5'->3')
ZmASR1 MZ00036717 MZ00042848 MZ00042852	GRMZM2G136910	ABA-, stress- and ripening induced protein 1	Transcription factor and/or chaperone-like activity	qRT-PCR	ZmASR1-F-q	95	GTCCCTCCCCGTGTGCTA
					ZmASR1-R-q		TGCATCACACGAGCGCATA
				mapping	ZmASR1-F-m	179	TGTCGATCCAATTGTCACTT
					ZmASR1-R-m		CGTGTACTCGGCGGACTC
ZmASR2	GRMZM2G057410	ABA-, stress- and ripening induced protein 2	Transcription factor and/or chaperone-like activity	qRT-PCR	ZmASR2-F-q	84	CCTCTTCGGCTGACCGTAGT
					ZmASR2-R-q		AGAATTAAACAGGTGTGTGGTTGTG
ZmASR3	GRMZM2G044132	ABA-, stress- and ripening induced protein 3	Transcription factor and/or chaperone-like activity	qRT-PCR	ZmASR3-F-q	152	ACCACCAACGACGACGAATA
					ZmASR3-R-q		CGGGAGGAGCCGTACTCT
				mapping	ZmASR3-F-m	1033	CTGCAAAGCAGCAAGCTCTA
					ZmASR3-R-m		GATCAGCCGAAGAAGTGGTG
ZmASR4	GRMZM2G168552	ABA-, stress- and ripening induced protein 4	Transcription factor and/or chaperone-like activity	qRT-PCR	ZmASR4-F-q	109	CGGCAGGGCCATGTACTC
					ZmASR4-R-q		GTCGTCCACGTTGTCGTAGTACTC
				mapping	ZmASR4-F-m	634	AGGGCCATGTACTCCAACAC
					ZmASR4-R-m		TGGGATGATCAGTCGTTTCA
ZmASR5	GRMZM2G052100	ABA-, stress- and ripening induced protein 5	Transcription factor and/or chaperone-like activity	qRT-PCR	ZmASR5-F-q	77	CCAGTTCCAGTTGTGCCATTG
					ZmASR5-R-q		GAAGAAACCGTGGTGCCTCAT
				mapping	ZmASR5-F-m	292	GTAGCGACGCGTTCCTGT
					ZmASR5-R-m		GGCTCCTCCCTCAAATGCTTC
ZmASR6	GRMZM2G057841	ABA-, stress- and ripening induced protein 6	Transcription factor and/or chaperone-like activity	mapping	ZmASR6-F-m	400	ATGGCTGAGGAGAAGAAG
					ZmASR6-R-m		TTCTTCTGGTGGTGCTCGT
ZmASR7-1	GRMZM2G014797	ABA-, stress- and ripening induced protein 7-1	Transcription factor and/or chaperone-like activity	qRT-PCR	ZmASR7-1-F-q	131	ACGAGCACCACCAGAAGAAAGA
					ZmASR7-1-R-q		GGTCGGTGCATATGTATGAACG
ZmASR7-2	GRMZM2G314075	ABA-, stress- and ripening induced protein 7-1	Transcription factor and/or chaperone-like activity	RT-PCR	ZmASR7-2-F-q	102	CACCGAGCGTCGATTTATCT
					ZmASR7-2-F-q		ATATACTAGGACGTTACGAAC
ZmASR7-3	GRMZM2G383699	ABA-, stress- and ripening induced	Transcription factor and/or	RT-PCR	ZmASR7-3-F-q	56	CCAACGACTGAAACAATGGC
					ZmASR7-3-F-q		TCTCCTCCATGGTGCTTGTT

		protein 7-1	chaperone-like activity				
ZmSPL14 MZ00000739	GRMZM2G169270	AtSPL14-like protein	Transcription factor	qRT-PCR	MZ00000739-F MZ00000739-R	84	GAGCAGAGTTGGAACATGTCATG TCGACATTTTGTGCATTGCA
ZmWD40.1 MZ00022082	GRMZM2G405690	WD40 repeat-like-containing domain protein	Unknown	qRT-PCR	MZ00022082-F MZ00022082-R	71	TTTATATCTCCAACAAGGCGTCTTT TCAGCAGTTGCCAGGACAAG
ZmUSPA.1 MZ00024643	GRMZM2G119258	USPA domain protein 1	Unknown	qRT-PCR	MZ00024643-F MZ00024643-R	64	TGAGCGAGTTCTGCGTTAAGC TCGGTAGCGTTCCGTTTTATG
ZmAHAS1	GRMZM2G143357	Acetohydroxyacid synthase 1	BCAA biosynthesis	qRT-PCR	ZmAHAS2-F ZmAHAS2-R	75	TTGGTATGCATGGCACAGTGTA ACCGCACACCAAATGCAA
ZmAHAS2	GRMZM2G007647	Acetohydroxyacid synthase 2	BCAA biosynthesis	qRT-PCR	ZmAHAS4-F ZmAHAS4-R	76	TGGTGCAACAGCCCGTTT CGGTTTTTTTGGTAATGCCTCTA
ZmAHAS3	GRMZM2G077215	Acetohydroxyacid synthase 3	BCAA biosynthesis	qRT-PCR	ZmAHAS5-F ZmAHAS5-R	73	CAGACATTACACTGCGCGATTT AATGATTCCTCCAGCTCCATTC
ZmKARI1	GRMZM2G161868	Ketolacid reductoisomerase 1	BCAA biosynthesis	qRT-PCR	ZmKARI1-F ZmKARI1-R	66	TTTGTGCGACTGTTTGTAAGTCAAG CCGGGTCCTCTGATAGAAGCT
ZmKARI2	GRMZM2G004382	Ketolacid reductoisomerase 2	BCAA biosynthesis	qRT-PCR	ZmKARI2-F ZmKARI2-R	65	CCGCTGATGCTGATTTCGT CACTGCGGATCCATACAAGCT
ZmDHAD1	GRMZM2G014069	Dihydroxyacid dehydratase 1	BCAA biosynthesis	qRT-PCR	ZmDAHD1-F ZmDHAD1-R	184	GAGATCGAGGCAAAAACAGG GGTTTTGGGTTGTGAATTGG
ZmDHAD2	AC234528.1_FGP005	Dihydroxyacid dehydratase 2	BCAA biosynthesis	qRT-PCR	ZmDHAD2-F ZmDHAD2-R	79	TAGTTCGGTTTTGCATGTGG TCAGCAGTTTCTGCAGCATT
ZmIPMI-lsu1	GRMZM2G370852	Isopropylmalate isomerase large subunit 1	BCAA biosynthesis	qRT-PCR	ZmIPMI-lsu1-F ZmIPMI-lsu1-R	87	CGTGCCTGCTGATGAAACTA CTGGCCTCAGCATCACTGTA
ZmIPMI-lsu2/3	GRMZM2G010044 GRMZM2G133988	Isopropylmalate isomerase large subunit 2/3	BCAA biosynthesis	qRT-PCR	ZmIPMI-lsu2/3-F ZmIPMI-lsu2/3-R	115	TGGTGCGACCTACAAATCAA AACACCGTTCTTTCCACCAG
ZmIPMI-ssu	GRMZM5G840002	Isopropylmalate isomerase small subunit	BCAA biosynthesis	qRT-PCR	ZmIPMI-ssu-F ZmIPMI-ssu-R	91	CCTCTGCGGAGATGAAGAAG GGCCGCAACTTATTTTGAGA
ZmIPMDH1	GRMZM2G803490	Isopropylmalate dehydrogenase 1	BCAA biosynthesis	qRT-PCR	ZmIPMDH1-F ZmIPMDH1-R	68	GCTCCGTGCCGGACTTG CATCTACCAACTGCGGCAATAC
ZmIPMDH2/3	GRMZM2G104613 GRMZM2G109935	Isopropylmalate dehydrogenase 2 and 3	BCAA biosynthesis	qRT-PCR	ZmIPMDH2/3-F ZmIPMDH2/3-R	68	GCAAAAGTCGCCGTTGGA TCTACAGTGTACAGTCTCGCAATCTG
ZmBCAT1	GRMZM2G071208	Branched-chain	BCAA	qRT-PCR	ZmBCAT1-F	77	TGTACACTTCACTGACGAGTCTTCAG

		aminotransferase 1	biosynthesis		ZmBCAT1-R		CGGCCAACTAATTCAGTTGCA
ZmBCAT2	GRMZM2G153536	Branched-chain aminotransferase 2	BCAA biosynthesis	qRT-PCR	ZmBCAT2-F ZmBCAT2-R	87	CCCGAGTACACCTTCCTCATCT GTCATGCACCACCAGGTTGA
ZmBCAT3	GRMZM2G055899	Branched-chain aminotransferase 3	BCAA biosynthesis	qRT-PCR	ZmBCAT3-F ZmBCAT3-R	80	TCATTGAAGTTGCTCAGAGCAAA TTCATCAGCGTTAATCAACTCATCT
ZmBCAT4	GRMZM2G047347	Branched-chain aminotransferase 4	BCAA biosynthesis	qRT-PCR	ZmBCAT4-F ZmBCAT4-R	68	GGGTTCCGGAGCCAATGT ATAGGGTATGAGATAGGAGAGCTGC TA
ZmBCAT5	GRMZM2G128547	Branched-chain aminotransferase 5	BCAA biosynthesis	qRT-PCR	ZmBCAT5-F ZmBCAT5-R	83	GGAAGGTTTAGCACCAATAAATTTG TGGTCTTCACACCCCCAGTAC
ZmGolS(1-4)	GRMZM2G120365 GRMZM2G165919 GRMZM2G131697 GRMZM2G141291	Galactinol synthase 1, 2, 3 and 4	RFO biosynthesis	qRT-PCR	ZmGolS1-4-F ZmGolS1-4-R	76	GAGGTTCACGGGCAAGGA GTAGATGTCCCACCACTTGTTCAC
ZmRafS MZ00036333	GRMZM2G340656	Raffinose synthase	RFO biosynthesis	qRT-PCR	MZ00036333-F MZ00036333-R	86	AATTACCCTCACGCGAAGCA AAGAATCAAATCACCGACCAAGA
ZmArginase	GRMZM2G174671	Arginase	Pro metabolism	qRT-PCR	ZmArginase1-F ZmArginase1-R	76	CGGGACAGGGATGCTAAGC CACTGGGTACGCCCTTGGTA
ZmOAT1	GRMZM2G095221	Orn-δ-transferase 1	Pro metabolism	qRT-PCR	ZmOAT1-F ZmOAT1-R	75	TGGAAGTACATTCGGTGGGAAT CCTTCGTCTCTGACCACTTTCA
ZmOAT2	GRMZM2G119583	Orn-δ-transferase 2	Pro metabolism	qRT-PCR	ZmOAT2-F ZmOAT2-R	65	CGCTCATCGTCTCGGAGAA CGCCGGTAGACAGTCCCTTA
ZmP5CS1	GRMZM2G061777	Δ^1-pyrroline-5-carboxylate synthetase 1	Pro metabolism	qRT-PCR	ZmP5CS2-F ZmP5CS2-R	73	TTAGTGCATGTGAGATGGCTGTT CGCTCATCCGACGACAAATT
ZmP5CS2	GRMZM2G375504	Δ^1-pyrroline-5-carboxylate synthetase 2	Pro metabolism	qRT-PCR	ZmP5CS1-F ZmP5CS1-R	76	CATTGAAGCCAGAAAAGATAGCAA TGGTTGATTGGGTCTTCCATATT
ZmP5CS3	GRMZM2G028535	Δ^1-pyrroline-5-carboxylate synthetase 3	Pro metabolism	qRT-PCR	ZmP5CS3-F ZmP5CS3-R	73	GATCCTGCCCGTGCATTC ACAACGAGACAGGTAGGCCAAT
ZmP5CR	GRMZM2G068665	Δ^1-pyrroline-5-carboxylate reductase	Pro metabolism	qRT-PCR	ZmP5CR-F ZmP5CR-R	67	CACGGCTGTCAGAAAAAAAGC TCCTGCAAATCTTGCATCTTGA
ZmProDH(1-2)	GRMZM2G117956 GRMZM2G053720	Pro dehydrogenase 1 and 2	Pro metabolism	qRT-PCR	ZmProDH-F ZmProDH-R	92	CGAGCGTGTGCATCAAGATC CGACGGGTGCCTCTTCTG
ZmGln1-2	GRMZM2G024104	Cytosolic Glu	Gln	qRT-PCR	ZmGln1-2-F	65	ACCGAGAAGGAAGGCAAAGG

		synthetase 1-2	biosynthesis		ZmGln1-2-R		ACGTACGGGTCCATGTTGGA
ZmGln1-3	GRMZM2G386046	Cytosolic Glu synthetase 1-3	Gln biosynthesis	qRT-PCR	ZmGln1-3-F ZmGln1-3-R	60	AGGGCAGTGGGAGTTCCAA CAGACCTGGTCGCCTGAAGA
ZmGln1-4	GRMZM2G036464	Cytosolic Glu synthetase 1-4	Gln biosynthesis	qRT-PCR	ZmGln1-4-F ZmGln1-4-R	75	TCGGACACCACAGAGAAGATCA GGCTTTGCTCCTGAGATCCAT
ZmGln2	GRMZM2G098290	Plastidic Glu synthetase 2	Gln biosynthesis	qRT-PCR	ZmGln2-F ZmGln2-R	73	CACTCCATTTGACCCTTGCTATT TGAAGGGCGATATGAGCAAAA
ZmGRP2	GRMZM2G080603	Glycine-rich RNA-binding protein 2	Nucleic acid binding	qRT-PCR	Endo1-F-ol 841 Endo1-R-ol 842	94	CACAACGCCTTCAGCACCTA AAGGTGACGAAGCCGAAGC

[a]Identification number of the corresponding oligonucleotide deposited on the micro-array.
[b]Maize genome release 5a.59 of November 2010 (http://www.maizesequence.org). When it was not possible to design gene-specific primers, primers commons to the genes indicated in parentheses and of sufficient quality for qRT-PCR were designed.
[c]Manually improved annotation from SwissProt, GenBank, Trembl and InterPro databases.

Table S3. Sequence identity between individual *ZmASR* genes.

	ZmASR1	*ZmASR2*	*ZmASR3*	*ZmASR4*	*ZmASR5*	*ZmASR6*	*ZmASR7-1*	*ZmASR7-2*	*ZmASR7-3*
ZmASR1		82 74/88	25 23/68	36 26/59	56 51/64	54 49/64	32	44	44
ZmASR2			25 24/31	37 28/59	56 53/61	55 54/61	33	48	47
ZmASR3				30 28/66	21 17/52	21 18/54	15	22	22
ZmASR4					32 30/46	33 28/50	23	35	35
ZmASR5						72 79/86	44	60	61
ZmASR6							41	58	57
ZmASR7-1			Coding region %[a] Exon 1/exon 2 %[b]					70	70
ZmASR7-2									97
ZmASR7-3									

[a]Values indicate the percentage of sequence identity at the nucleotide level in the whole coding regions of the genes.
[b]Values indicate the percentage of sequence identity at the nucleotide level between individual exons.

Table S4. Summary of exon lengths of various *ASR* genes from Poaceae and properties of their deduced amino acid sequences.

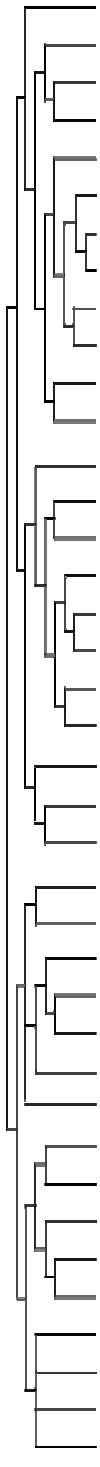

Gene name	Exon 1 from ATG[a]	Exon 2 to STOP[a]	Disorder-promoting amino acis[b]	His-rich domain	NLS[c]	First Zn^{2+}-binding site[d]	Zn^{2+}-dependent DNA-binding site[d]	Sequence hindering DNA-binding[d]
PeASR5	NA	NA	70.3	Yes	Bipartite	59(59)	86(100)	90(100)
BdASR2	231	189	63.7	Yes	Bipartite	65(71)	71(100)	90(90)
HvASR1	129	81	59.4	Yes	Bipartite	76 (82)	ND (ND)	ND (ND)
HvASR2	231	186	58.7	Yes	Bipartite	76 (82)	71 (100)	90 (90)
OsASR5	231	186	46.8	Yes	Bipartite	76 (76)	71 (100)	90 (100)
SbASR1	252	186	50.7	Yes	Bipartite	82 (82)	81 (100)	90 (100)
SoDIP22	243	186	63.4	Yes	Bipartite	76 (76)	86 (100)	90 (100)
ZmASR1	231	186	62.3	Yes	Bipartite	82 (82)	86 (100)	90 (100)
SbASR2	216	189	49.6	Yes	Bipartite	65 (65)	86 (100)	90 (100)
ZmASR2	207	189	61.8	Yes	Bipartite	59 (65)	86 (100)	80 (90)
PeASR1	NA	NA	69.6	Yes	Bipartite	65(65)	71(100)	80(90)
PeASR2	NA	NA	69.3	Yes	Monopartite	53(65)	71(100)	80(90)
BdASR3	NA	NA	73.6	No	Bipartite	12(29)	71(100)	80(100)
HvASR3	609	210	65.1	No	Bipartite	5.5 (22)	71 (100)	70 (100)
TaASR	NA	NA	74.2	No	Bipartite	16(26)	71(100)	80(100)
OsASR4	459	231	47.2	No	Bipartite	11 (22)	57 (86)	80 (100)
SbASR3	603	207	42.4	No	Bipartite	11 (22)	71 (86)	80 (100)
ZmASR3	594	216	66.9	No	Bipartite	11 (22)	71 (86)	80 (100)
PeASR3	NA	NA	74.1	No	Bipartite	11(21)	57(86)	70(100)
PeASR4	NA	NA	73.0	No	Bipartite	16(26)	57(86)	70(100)
ZmASR4	202	206	64.4	No	No	5.8 (5.8)	28 (57)	70 (100)
BdASR4	414	192	65.7	No	No	11(26)	57(71)	70(100)
OsASR6	345	204	53.3	Yes	Monopartite	17 (17)	57 (71)	40 (50)
SbASR5	153	153	47.4	Yes	Monopartite	70 (82)	57 (71)	80 (90)
ZmASR5	162	153	61.5	Yes	Monopartite	70 (76)	57 (71)	80 (90)
OsASR3	159	159	51.5	Yes	Monopartite	67 (67)	57 (71)	80 (90)
SbASR4	171	153	52.5	Yes	Monopartite	50 (67)	71 (71)	80 (90)
ZmASR6	168	153	64.1	Yes	Monopartite	56 (56)	71 (86)	80 (90)
PeASR6	NA	NA	68.1	Yes	Monopartite	59(59)	71(86)	80(90)
PeASR7	NA	NA	67.0	Yes	Monopartite	59(65)	71(86)	80(90)
BdASR5	168	168	67.3	Yes	Monopartite	12(18)	71(71)	70(80)
BdASR6	NA	NA	69.8	No	Monopartite	6(12)	71(71)	50(60)
OsASR2	150	168	71.1	No	Monopartite	23 (35)	71 (71)	60 (70)
OsASR1	135	156	59.3	No	Monopartite	5.5 (5.5)	71 (71)	60 (70)
SbASR6	0	261	46.3	Yes	No	35 (47)	71 (71)	ND (ND)
SbASR7	0	306	59.4	Yes	Monopartite	23 (23)	86 (86)	70 (80)
ZmASR7-1	0	321	67.9	Yes	No	23 (29)	ND (ND)	ND (ND)
ZmASR7-2	0	309	55.9	Yes	Monopartite	23 (29)	86 (86)	70 (80)
ZmASR7-3	0	309	59.9	Yes	Monopartite	23 (29)	86 (86)	80 (90)

[a]Exon lengths (bp) of *ASR* genes from Poaceae. "NA" annotation stands for "non accessible".
[b]Percentage of disorder-promoting amino acid residues according to Romero et al. (2001).
[c]Bipartite NLS lacking the last Lys of the A region from the LLA23 protein (Wang et al., 2005).
[d]Percentage of sequence identity (similarity) between various Poaceae ASR proteins and SlASR1 protein (Rom et al., 2006). "ND" annotation stands for "non determined".

Table S5. *ZmASR* 1-OE plants maintain kernel yield under water-limited conditions.

	WT				*ZmASR1*-OE						*P*[b]						
	Control		Deficit		Control		Deficit		Ratio *ZmASR1*-OE/WT		Analysis of variance table			Analysis of Bonferroni method			
	Mean[a]	SE[a]	Mean[a]	SE[a]	Mean[a]	SE[a]	Mean[a]	SE[a]	Control	Deficit	*ZmASR1*-OE	Deficit	Interaction	Pair tested	Difference	Lower	Upper
Total chlorophyll content (mg g^{-1} FW)	1.6	0.08	1.16	0.07	1.77	0.16	1.4	0	1.11	1.21	0.0634	0.0057	0.749	NR	NR	NR	NR
Dry leaf weight (g g^{-1} FW)	0.2	0.01	0.19	0.01	0.23	0.03	0.24	0.01	1.15	1.26	0.058	0.8139	0.6197	NR	NR	NR	NR
Ear leaf area (cm^2)	428.94	3.99	322.37	3.87	443.03	4.04	336.46	3.83	1.03	1.04	0.002	<2.2E-16	0.222	NR	NR	NR	NR
Shoot biomass (g $plant^{-1}$)	85.68	2.31	51.66	2.24	95.77	2.31	52.05	2.2	1.12	1.01	NR	NR	0.0336	*ZmASR1*-OE.Deficit - *ZmASR1*-OE.Control	-43.72	-52.22	-35.22
														ZmASR1-OE.Deficit - WT.Control	-33.63	-42.13	-25.13
														ZmASR1-OE.Control - WT.Deficit	44.11	35.53	52.68
														ZmASR1-OE.Control - WT.Control	10.08	1.39	18.78
														WT.Deficit - WT.Control	-34.02	-42.60	-25.45
Shoot biomass yield (t/ha)	6.85	0.18	4.13	0.18	7.66	0.18	4.16	0.18	1.12	1.01	NR	NR	0.0336	*ZmASR1*-OE.Deficit - *ZmASR1*-OE.Control	-34.97	-41.77	-28.17
														ZmASR1-OE.Deficit - WT.Control	-26.91	-33.71	-20.11
														ZmASR1-OE.Control - WT.Deficit	35.28	28.42	42.14
														ZmASR1-OE.Control - WT.Control	8.07	1.11	15.02
														WT.Deficit - WT.Control	-27.22	-34.08	-20.36
Kernel weight (g $plant^{-1}$)	85.9	1.43	37.09	1.39	92.13	1.42	43.32	1.378	1.07	1.17	0.0002	<2.2E-16	0.4648	NR	NR	NR	NR
Kernel dry weight (t ha^{-1})	5.85	0.1	2.54	0.1	6.28	0.1	2.97	0.1	1.07	1.17	0.0002	<2.2E-16	0.6435	NR	NR	NR	NR
Kernel number ($plant^{-1}$)	292.28	5.56	173.09	5.45	321	5.56	201.81	5.39	1.10	1.17	9.80E-06	<2.2E-16	0.4993	NR	NR	NR	NR
Harvest index (%)	50.1	0.89	42.37	0.87	49.58	0.89	45.11	0.85	0.99	1.06	NR	NR	0.0649	*ZmASR1*-OE.Deficit - *ZmASR1*-OE.Control	-4.46	-7.76	-1.17
														ZmASR1-OE.Deficit - WT.Control	-4.99	-8.28	-1.69
														ZmASR1-OE.Control - WT.Deficit	7.21	3.88	10.53
														WT.Deficit - WT.Control	-7.73	-11.05	-4.40

[a]Mean and SE values of WT and *ZmASR1*-OE plants.

[b]Field physiology and yield performance measurements were categorized as *ZmASR1*-OE (light-gray box), deficit (gray box) and interaction (dark-gray box) as follows. *ZmASR1*-OE: measurements that showed significant ($P < 0.05$) changes in *ZmASR1*-OE plants compared to WT plants when the additive model could be retained. Deficit: measurements that showed significant ($P < 0.05$) changes under water deficit conditions compared to well-watered conditions when the additive model could be retained. Interaction: measurements that showed significant ($P < 0.05$) changes in *ZmASR1*-OE plants compared to WT plants by the Bonferroni method when the additive model could not be retained. Experimental details are described in Methods. NR: not relevant.

Table S6. Proteins that showed significant changes in *ZmASR1* -OE leaves compared to WT leaves, their annotated function, location and quantification.

											WT				*ZmASR1* -OE			
											Control		Deficit		Control		Deficit	
Spot ID[a]	Maize gene model[b]	Annotation[c]	Location[d]	*M*r (10^3)[e]	pI[e]	*M*r (10^3)[f]	pI[f]	Spectre match no.	Peptide match no.	PAI[g]	Mean[h]	SE[h]	Mean[h]	SE[h]	Mean[h]	SE[h]	Mean[h]	SE[h]
s0732	NI	ND	ND	ND	ND	66.5	4.9	ND	ND	ND	204.06	1.81	527.55	ND	202.41	14.4	178.24	38.96
s1021	GRMZM2G019121	Class II Aspartyl-tRNA synthetase (AspRS)	Cytoplasm, plastid	58.7	6.8	60.0	6.4	7	6	0.27	104.24	7.555	78.12	0.335	135.03	25.34	173.63	0.96
s1202	GRMZM2G008247	β-D-glucosidase (GLU)	Plastid	58.6	6.0	56.1	5.8	19	16	0.91	35.05	17.075	61.08	16.29	102.89	21.43	106.30	16.045
	GRMZM2G034152	Flavin containing amine oxidase		52.0	5.6	56.1	5.8	3	3	0.14								
s1388	GRMZM2G127393	Trigger factor-like protein	Plastid stroma	52.1	5.0	52.3	4.8	8	8	0.28	134.36	0.545	111.12	24.735	67.15	1.695	60.68	12.445
s1406	GRMZM2G123204	Adenylosuccinate synthetase (AdSS)	Plastid stroma	48.9	5.9	51.6	5.8	4	4	0.18	122.75	18.84	50.29	18.925	15.56	1.09	36.64	5.305
	GRMZM2G020446	Diaminopimelate decarboxylase		48.4	6.1	51.6	5.8	2	2	0.09								
s1422	GRMZM2G123204	Adenylosuccinate synthetase (AdSS)	Plastid stroma	48.9	5.9	51.3	6.1	8	7	0.36	311.28	35.235	131.56	33.695	131.28	0.615	129.24	24.585
s1442	NI	ND	ND	ND	ND	50.8	5.9	ND	ND	ND	66.79	11.69	44.62	7.335	17.19	1.465	25.17	6.105
s1444	GRMZM2G449496	Plastid transcriptionally active 16 (PTAC16)	Plastid nucleoid	49.5	5.1	50.7	5.9	16	15	0.73	292.34	8.19	305.67	12.74	194.21	18.995	225.32	32.905
s1612	GRMZM2G104613	3-isopropylmalate dehydrogenase 2 (IPMDH2)	Plastid stroma	39.3	5.0	47.2	4.9	5	5	0.31	81.35	1.765	57.95	2.735	30.36	4.285	50.07	0.325
	GRMZM2G803490	3-isopropylmalate dehydrogenase 1 (IPMDH1)		39.1	5.0	46.5	4.8	2	2	0.13								
s1641	GRMZM2G803490	3-isopropylmalate dehydrogenase 1 (IPMDH1)	Plastid stroma	39.1	5.0	46.5	4.8	3	3	0.20	187.14	17.83	101.93	8.55	90.32	11.95	89.56	7.73
s1886	GRMZM2G097226	Pyruvate dehydrogenase subunit E1β (PDH-E1β)	Mitochondria	37.3	5.1	40.6	5.0	7	5	0.70	144.21	19.12	125.94	21.39	98.18	5.06	81.78	5.285
s1904	AC147602.5_FGP004	Sedoheptulose-1,7-bisphosphatase (SBPase)	Plastid stroma	37.7	5.5	40.2	4.7	19	15	0.95	996.16	86.8	752.43	33.985	693.40	109.79	477.21	18.56
s1913	GRMZM2G102838	Photosystem II stability/assembly factor, HCF136 type (HCF-136)	Thylakoid-peripheral-lumenal-side	40.2	6.0	40.0	5.3	21	17	1.05	663.49	11.265	813.33	39.005	754.16	6.42	552.43	1.985
s2020	AC210204.3_FGP002	C2 domain containing protein	ND	32.7	5.1	37.8	4.9	7	7	0.88	93.49	2.655	103.23	5.81	92.72	2.47	52.00	8.74
s2141	NI	ND	ND	ND	ND	35.0	4.8	ND	ND	ND	14.52	0.875	16.78	1.235	4.37	1.985	11.49	1.105
s2210	GRMZM2G018375	Thiazole biosynthetic enzyme 1-1 (THI1)	Plastid stroma	33.0	4.9	33.6	4.9	12	8	1.18	260.21	57.9	253.72	24.85	185.99	0.555	96.00	7.315
s2275	GRMZM2G064163	Spermidine synthase 1	ND	28.0	5.2	32.2	5.1	11	8	1.09	78.25	13.1	48.86	7.02	142.19	3.935	60.22	12.19
s2316	GRMZM2G078566	Glucan endo-1,3-β-glucosidase 5	Plasma membrane	31.7	4.7	31.3	5.2	2	2	0.13	53.57	1.325	45.08	6.13	83.79	0.46	58.27	6.515
s2322	NI	ND	ND	ND	ND	31.3	5.1	2	2	0.67	30.89	0.65	33.69	4.005	54.14	3.65	45.08	1.775
s2460	NI	ND	ND	ND	ND	28.6	5.4	2	2	0.15	49.26	1.225	82.59	4.525	40.53	9.415	51.94	2.44
s2528	GRMZM2G068244	NAD-dependent epimerase/dehydratase	Plastid stroma	27.7	6.8	26.7	6.5	2	2	0.17	177.51	5.515	210.01	36.29	273.89	9.41	253.79	7.15
s3353	NI	ND	ND	ND	ND	13.6	5.4	ND	ND	ND	23.55	0.9	24.78	1.84	43.47	6.075	32.76	3.155

[a]Identification number of the corresponding protein spot on the 2-D reference map showing significant ($P < 0.05$) changes in *ZmASR1* -OE leaves compared to WT leaves under both treatment conditions and manually evaluated from the 2-D reference map.

[b]Maize genome release 5a.59 of November 2010 (http://www.maizesequence.org). "NI" stands for "not identified by LC-MS/MS".

[c]Manually improved annotation from SwissProt, GenBank, Trembl and InterPro databases. Annotations in gray were eliminated based on the absence of correspondence between the theorical *M*r and the observed *M*r and/or the PAI. "ND" stands for "not determined".

[d]Manually improved cellular locations from experimental data (Majeran et al. 2010).

[e]Observed *M*r and pI.

[f]Theorical *M*r and pI.

[g]Protein Abondance Index.

[h]Mean and SE values of a biological duplicate.

Table S7. Unique metabolites identified in *ZmASR1*-OE and WT leaves. Values represent the mean (log_{10}) of biological duplicates ± SE.

	WT				*ZmASR1*-OE			
	Control		Deficit		Control		Deficit	
	Mean	SE	Mean	SE	Mean	SE	Mean	SE
Bishydroxybutyrate	-2.63	0.04	-2.77	0.05	-2.79	0.05	-2.83	0.00
α-Hydroxyglutarate	-3.12	0.10	-3.40	0.01	-3.35	0.07	-3.41	0.07
Ala	0.05	0.04	-0.05	0.04	-0.03	0.06	-0.14	0.01
α-Ketoglutarate	-2.05	0.05	-2.30	0.04	-2.16	0.04	-2.36	0.03
Arabinose	-2.17	0.04	-2.04	0.04	-2.32	0.04	-2.08	0.01
Ascorbate	-1.83	0.06	-2.10	0.10	-1.99	0.13	-2.04	0.03
Asn	-2.88	0.06	-2.94	0.08	-3.00	0.02	-3.14	0.05
Asp	-1.25	0.06	-1.45	0.03	-1.28	0.06	-1.52	0.02
β-Ala	-2.37	0.06	-2.34	0.03	-2.40	0.04	-2.40	0.03
Benzoate	-3.14	0.09	-3.07	0.04	-3.24	0.03	-3.19	0.05
β-Sitosterol	-3.15	0.10	-3.32	0.13	-3.30	0.17	-3.21	0.16
Citramalate	-3.06	0.01	-3.26	0.06	-3.15	0.06	-3.44	0.05
Citrate	-2.26	0.05	-2.40	0.04	-2.37	0.05	-2.49	0.01
Cys	-3.20	0.03	-3.09	0.04	-3.18	0.06	-3.14	0.03
Decanoate	-3.16	0.10	-3.89	0.40	-3.68	0.32	-3.46	0.04
Dehydroascorbate	-1.02	0.03	-1.02	0.03	-1.11	0.03	-1.03	0.03
Digalactosylglycerol	-1.10	0.03	-1.19	0.05	-1.17	0.04	-1.25	0.03
Dopamine	-2.33	0.04	-2.11	0.03	-2.34	0.04	-2.11	0.02
Ethanolamine	-1.16	0.06	-1.08	0.03	-1.22	0.04	-1.13	0.02
Ethylphosphate	-2.95	0.22	-2.61	0.08	-2.90	0.14	-2.74	0.22
Fructose	-0.02	0.04	0.25	0.05	-0.12	0.06	0.18	0.05
GABA	-4.23	0.32	-3.88	0.24	-4.69	0.03	-3.98	0.41
Galactinol	-2.36	0.04	-2.14	0.02	-2.48	0.04	-2.22	0.02
Galactose	-1.38	0.04	-1.07	0.04	-1.46	0.05	-1.12	0.02
Galactosylglycerol	-0.23	0.03	-0.39	0.05	-0.32	0.04	-0.46	0.04
Gln	-1.61	0.05	-1.74	0.03	-1.68	0.03	-1.86	0.02
Glu	-1.53	0.05	-1.60	0.03	-1.58	0.05	-1.67	0.03
Glucarate	-3.30	0.06	-3.15	0.03	-3.35	0.10	-3.16	0.02
Glucose	-0.08	0.03	0.25	0.03	-0.25	0.05	0.17	0.02
Gly	-1.53	0.03	-1.42	0.03	-1.65	0.06	-1.53	0.04
Glycerate	-1.43	0.04	-1.34	0.03	-1.52	0.06	-1.44	0.02
Glycerol	-1.41	0.04	-1.36	0.05	-1.42	0.05	-1.41	0.07
HSer	-3.18	0.10	-3.38	0.02	-3.24	0.10	-3.51	0.04
Ile	-2.15	0.04	-2.01	0.04	-2.25	0.05	-2.16	0.01
Lactate	-3.40	0.28	-4.60	0.01	-3.09	0.36	-2.78	0.29
Lactose	-2.83	0.03	-2.81	0.01	-2.96	0.08	-2.86	0.02
Laurate	-3.89	0.45	-4.24	0.36	-4.51	0.17	-4.14	0.34
Leu	-2.06	0.04	-1.87	0.03	-2.14	0.04	-2.02	0.01
Linoleate	-3.36	0.04	-3.59	0.05	-3.42	0.04	-3.57	0.09
Linolenate	-2.60	0.08	-2.84	0.03	-2.75	0.04	-2.88	0.09
Lys	-3.37	0.15	-3.36	0.16	-3.23	0.20	-3.63	0.02
Maleate	-3.08	0.05	-3.05	0.05	-3.06	0.08	-3.10	0.03
Malate	-1.33	0.05	-1.49	0.05	-1.44	0.06	-1.59	0.01
Mannose	-2.77	0.05	-2.53	0.05	-3.16	0.15	-2.58	0.03
Melibiose	-2.97	0.06	-2.61	0.03	-3.18	0.14	-2.73	0.05
Met	-2.99	0.04	-2.98	0.04	-3.02	0.07	-2.96	0.01
Monomethylphosphate	-2.34	0.07	-2.44	0.04	-2.50	0.12	-2.65	0.08
Myo-inositol	-1.20	0.03	-1.25	0.05	-1.31	0.05	-1.28	0.03
Nicotinate	-2.79	0.01	-2.66	0.03	-2.82	0.02	-2.75	0.09
Nonanoate	-3.12	0.08	-3.11	0.02	-3.18	0.05	-3.35	0.04
O-AcetylSer	-2.87	0.02	-2.87	0.05	-2.89	0.06	-2.95	0.04
Octanoate	-3.24	0.09	-3.24	0.07	-3.29	0.06	-3.61	0.01
Orn	-2.48	0.05	-2.62	0.03	-2.50	0.08	-2.72	0.03
Palmitate	-1.57	0.06	-1.81	0.07	-1.78	0.12	-1.74	0.02
Phe	-2.67	0.03	-2.47	0.03	-2.72	0.05	-2.59	0.01
Phosphate	-1.95	0.04	-1.87	0.03	-2.03	0.06	-1.93	0.01
Pipecolate	-2.82	0.11	-2.93	0.05	-2.71	0.11	-2.84	0.06
Pro	-1.85	0.04	-1.71	0.03	-1.92	0.04	-1.79	0.01
PyroGlu	-2.57	0.05	-2.66	0.03	-2.63	0.03	-2.71	0.01
Pyruvate	-1.24	0.04	-1.43	0.04	-1.33	0.04	-1.52	0.02
Quinate	-1.36	0.04	-1.01	0.07	-1.51	0.06	-1.06	0.02
Raffinose	-1.84	0.04	-1.49	0.04	-1.96	0.04	-1.53	0.01
Rhamnose	-2.75	0.03	-2.89	0.04	-2.85	0.05	-2.90	0.04
Ribose	-1.64	0.03	-1.52	0.04	-1.70	0.04	-1.61	0.06
Ser	-1.49	0.05	-1.40	0.03	-1.51	0.05	-1.49	0.02
Shikimate	-1.20	0.03	-0.81	0.05	-1.34	0.05	-0.83	0.02
Sinapinate	-3.49	0.05	-3.33	0.10	-3.58	0.03	-3.47	0.11
Sorbitol	-3.96	0.69	-4.60	0.01	-4.69	0.03	-3.58	0.66
Spermidine	-3.27	0.03	-3.39	0.06	-3.44	0.09	-3.50	0.09
Stearate	-4.64	0.02	-4.60	0.01	-4.40	0.27	-4.19	0.51
Succinate	-2.68	0.07	-2.67	0.04	-2.75	0.06	-2.73	0.01
Sucrose	0.07	0.03	0.09	0.03	-0.07	0.04	0.01	0.02
T-Aconitate	-0.15	0.04	-0.14	0.05	-0.37	0.04	-0.24	0.03
T-Caffeate	-3.61	0.34	-3.20	0.09	-3.67	0.33	-3.19	0.08
T-Caffeoylquinate	-2.80	0.02	-2.90	0.03	-2.93	0.06	-3.06	0.03
Tetradecanoate	-2.23	0.03	-2.13	0.02	-2.37	0.09	-2.16	0.03
Thr	-2.30	0.05	-2.26	0.03	-2.35	0.03	-2.32	0.02
Threitol	-2.58	0.05	-2.59	0.03	-2.66	0.06	-2.63	0.01
Threonate	-2.55	0.07	-2.64	0.02	-2.65	0.07	-2.58	0.07
Threonate-1,4-lactone B	-2.93	0.06	-2.99	0.02	-2.99	0.08	-2.98	0.06
Trp	-2.64	0.03	-2.48	0.03	-2.75	0.05	-2.63	0.03
Urea	-3.60	0.22	-3.96	0.31	-3.23	0.16	-2.74	0.25
Val	-1.81	0.04	-1.76	0.03	-1.91	0.04	-1.87	0.01
Xylose	-2.19	0.02	-2.11	0.06	-2.32	0.05	-2.14	0.02

Table S8. Within-groups correlation matrix. Correlations were calculated from residual data. Significant correlations at P < 0.05 are indicated by dark shading. Green and Red distinguish negative and positive correlations, respectively.

Name	Total chlo	ZmASR1	ZmSPL14	ZmWD40	ZmUSPA	ZmArgina	ZmOAT1	ZmOAT2	ZmP5CS1	ZmP5CS2	ZmP5CS3	ZmP5CR	ZmProDH	ZmGln1-2	ZmGln1-3	ZmGln1-4	ZmGln2	ZmGolS(1	ZmRafS(	ZmAHAS1	ZmAHAS2	ZmAHAS3	ZmKARI1	ZmKARI2	ZmDHAD	ZmDHAD	ZmIPMS1	ZmIPMI-l
Total chlorophyll content	1.0000	-0.0896	0.2040	-0.0576	-0.2966	0.6255	0.2148	0.4501	0.0792	-0.2640	-0.4436	-0.0180	0.4468	-0.1800	-0.0727	0.3775	0.1060	0.2671	-0.2581	-0.6126	-0.2966	0.4774	-0.5247	-0.5237	0.2197	0.4476	-0.5011	-0.3752
ZmASR1	-0.0896	1.0000	0.1073	0.1870	0.5188	0.6063	0.3182	-0.2083	0.7035	0.4425	0.3161	0.2304	-0.6005	0.4609	0.7208	0.3839	0.6174	0.7427	-0.6358	0.6216	0.9678	0.3442	0.3366	0.0710	-0.3738	0.6136	0.0135	0.9425
ZmSPL14 (MZ00000739)	0.2040	0.1073	1.0000	-0.3975	0.0458	-0.1818	0.2635	-0.7806	-0.2201	0.1704	-0.0962	-0.1151	0.6880	0.2764	0.0344	0.2980	-0.2092	-0.2730	-0.2418	0.3549	-0.0482	0.0602	0.5125	0.3350	0.8412	0.6350	0.4727	0.0074
ZmWD40.1 (MZ00022082)	-0.0576	0.1870	-0.3975	1.0000	0.8117	0.2125	0.7686	0.2973	0.8078	0.7713	0.8485	0.9570	-0.5087	0.7214	0.7664	0.6976	0.8643	0.6467	-0.6768	-0.3503	0.1627	0.7751	-0.6384	-0.7956	-0.2004	-0.4416	-0.7832	0.0604
ZmUSPA.1 (MZ00024643)	-0.2966	0.5188	0.0458	0.8117	1.0000	0.0848	0.8444	-0.2704	0.8114	0.9876	0.9613	0.8975	-0.4628	0.9678	0.9385	0.7618	0.8366	0.5919	-0.8229	0.1943	0.4825	0.6853	-0.1051	-0.4011	0.0211	-0.0960	-0.3510	0.4307
ZmArginase	0.6255	0.6063	-0.1818	0.2125	0.0848	1.0000	0.2419	0.5253	0.6302	0.0014	-0.1177	0.1529	-0.3685	0.0363	0.4148	0.4054	0.5800	0.8375	-0.5232	-0.1577	0.4916	0.5546	-0.3520	-0.4592	-0.4634	0.5428	-0.5452	0.3930
ZmOAT1	0.2148	0.3182	0.2635	0.7686	0.8444	0.2419	1.0000	-0.1356	0.7449	0.8809	0.7552	0.9114	-0.0610	0.9110	0.8406	0.9794	0.8065	0.5801	-0.9239	-0.1786	0.1622	0.9210	-0.3795	-0.6698	0.3297	0.0651	-0.5719	0.0797
ZmOAT2	0.4501	-0.2083	-0.7806	0.2973	-0.2704	0.5253	-0.1356	1.0000	0.1995	-0.3588	-0.2242	0.0636	-0.3053	-0.4024	-0.1282	-0.0663	0.2098	0.3674	0.1027	-0.7342	-0.1950	0.2138	-0.8025	-0.6238	-0.6055	-0.3190	-0.7324	-0.2920
ZmP5CS1	0.0792	0.7035	-0.2201	0.8078	0.8114	0.6302	0.7449	0.1995	1.0000	0.7381	0.6959	0.7978	-0.6595	0.7250	0.9420	0.7632	0.9919	0.9493	-0.8800	0.0013	0.6373	0.8223	-0.3584	-0.6162	-0.3609	0.1132	-0.6445	0.5349
ZmP5CS2	-0.2640	0.4425	0.1704	0.7713	0.9876	0.0014	0.8809	-0.3588	0.7381	1.0000	0.9498	0.8937	-0.3200	0.9921	0.9012	0.7933	0.7756	0.4995	-0.8205	0.1755	0.3859	0.6873	-0.0829	-0.3853	0.1774	-0.0803	-0.3082	0.3416
ZmP5CS3	-0.4436	0.3161	-0.0962	0.8485	0.9613	-0.1177	0.7552	-0.2242	0.6959	0.9498	1.0000	0.8968	-0.4701	0.9039	0.8218	0.6287	0.7372	0.4373	-0.6566	0.1120	0.3280	0.5663	-0.1620	-0.3942	-0.0001	-0.3587	-0.3446	0.2853
ZmP5CR	-0.0180	0.2304	-0.1151	0.9570	0.8975	0.1529	0.9114	0.0636	0.7978	0.8937	0.8968	1.0000	-0.3351	0.8716	0.8379	0.8413	0.8628	0.6015	-0.8009	-0.2583	0.1587	0.8471	-0.5196	-0.7449	0.0517	-0.2904	-0.6872	0.0676
ZmProDH(1-2)	0.4468	-0.6005	0.6880	-0.5087	-0.4628	-0.3685	-0.0610	-0.3053	-0.6595	-0.3200	-0.4701	-0.3351	1.0000	-0.2351	-0.5360	-0.0307	-0.5982	-0.6536	0.2532	-0.2688	-0.7316	-0.1463	0.0689	0.1371	0.8664	0.1959	0.2680	-0.6870
ZmGln1-2	-0.1800	0.4609	0.2764	0.7214	0.9678	0.0363	0.9110	-0.4024	0.7250	0.9921	0.9039	0.8716	-0.2351	1.0000	0.9002	0.8397	0.7627	0.4980	-0.8590	0.1809	0.3771	0.7185	-0.0589	-0.3785	0.2590	0.0216	-0.2896	0.3333
ZmGln1-3	-0.0727	0.7208	0.0344	0.7664	0.9385	0.4148	0.8406	-0.1282	0.9420	0.9012	0.8218	0.8379	-0.5360	0.9002	1.0000	0.8244	0.9418	0.8145	-0.9323	0.1909	0.6468	0.7894	-0.1447	-0.4630	-0.1189	0.1560	-0.4448	0.5729
ZmGln1-4	0.3775	0.3839	0.2980	0.6976	0.7618	0.4054	0.9794	-0.0663	0.7632	0.7933	0.6287	0.8413	-0.0307	0.8397	0.8244	1.0000	0.8140	0.6552	-0.9552	-0.2044	0.1986	0.9600	-0.3991	-0.6919	0.3042	0.2208	-0.6048	0.1069
ZmGln2	0.1060	0.6174	-0.2092	0.8643	0.8366	0.5800	0.8065	0.2098	0.9919	0.7756	0.7372	0.8628	-0.5982	0.7627	0.9418	0.8140	1.0000	0.9191	-0.8961	-0.0880	0.5406	0.8719	-0.4349	-0.6902	-0.2862	0.0436	-0.7021	0.4332
ZmGolS(1-4)	0.2671	0.7427	-0.2730	0.6467	0.5919	0.8375	0.5801	0.3674	0.9493	0.4995	0.4373	0.6015	-0.6536	0.4980	0.8145	0.6552	0.9191	1.0000	-0.7953	-0.0436	0.6649	0.7634	-0.3802	-0.5937	-0.4901	0.2730	-0.6573	0.5556
ZmRafS (MZ00036333)	-0.2581	-0.6358	-0.2418	-0.6768	-0.8229	-0.5232	-0.9239	0.1027	-0.8800	-0.8205	-0.6566	-0.8009	0.2532	-0.8590	-0.9323	-0.9552	-0.8961	-0.7953	1.0000	-0.0189	-0.4792	-0.9153	0.2456	0.5720	-0.1057	-0.3380	0.5209	-0.3926
ZmAHAS1	-0.6126	0.6216	0.3549	-0.3503	0.1943	-0.1577	-0.1786	-0.7342	0.0013	0.1755	0.1120	-0.2583	-0.2688	0.1809	0.1909	-0.2044	-0.0880	-0.0436	-0.0189	1.0000	0.7023	-0.3847	0.9257	0.7789	-0.0689	0.4323	0.7605	0.7918
ZmAHAS2	-0.2966	0.9678	-0.0482	0.1627	0.4825	0.4916	0.1622	-0.1950	0.6373	0.3859	0.3280	0.1587	-0.7316	0.3771	0.6468	0.1986	0.5406	0.6649	-0.4792	0.7023	1.0000	0.1706	0.4080	0.1881	-0.5191	0.4665	0.1050	0.9904

Table S9. Number of individual significant correlations for the whole matrix and its submatrices.

		Individual significant correlations			
		Obtained			Expected[b]
Matrix[a]	Significance level	Total	Positive	Negative	Total
Whole matrix	$P < 0.05$	765	478	278	507
	$P < 0.01$	170	104	66	101
	$P < 0.001$	23	14	9	10
Transcript-transcript	$P < 0.05$	71	60	11	32
	$P < 0.01$	22	19	3	6
	$P < 0.001$	2	2	0	0
Spot protein-spot protein	$P < 0.05$	14	7	7	12
	$P < 0.01$	2	1	1	2
	$P < 0.001$	0	0	0	0
Metabolite-metabolite	$P < 0.05$	323	300	23	175
	$P < 0.01$	67	63	4	35
	$P < 0.001$	10	9	1	4
Transcript-spot protein	$P < 0.05$	35	13	22	40
	$P < 0.01$	8	4	4	8
	$P < 0.001$	1	0	1	1
Transcript-metabolite	$P < 0.05$	210	48	162	151
	$P < 0.01$	46	6	40	30
	$P < 0.001$	5	0	5	3
Transcript-TCC	$P < 0.05$	1	1	0	2
	$P < 0.01$	0	0	0	0
	$P < 0.001$	0	0	0	0
Spot protein-metabolite	$P < 0.05$	105	44	61	92
	$P < 0.01$	24	10	14	18
	$P < 0.001$	5	3	2	2
Spot protein-TCC	$P < 0.05$	1	0	1	1
	$P < 0.01$	0	0	0	0
	$P < 0.001$	0	0	0	0
Metabolite-TCC	$P < 0.05$	5	5	0	4
	$P < 0.01$	1	1	0	1
	$P < 0.001$	0	0	0	0

[a]TCC: total chlorophyll content.

[b]Number of expected individual significant correlations under the null hypothesis, with the number of positive and negative individual significant correlations following a symetric binomial distribution.

Table S10. Pair-wise correlations of ZmASR1 targets against BCAA-related ZmASR1 targets.

Analyses	Parameter x[a]	Trend in *ZmASR1* -OE	Parameter y[b]	corr(x,y)[c]
qRT-PCR	*ZmAHAS1*	Up	ZmKARI1	0.9257
	ZmBCAT4	Up	Ile	0.9263
			Leu	0.9451
			Val	0.9584
	ZmKARI1	Up	ZmAHAS1	0.9257
			ZmKARI2	0.9349
	ZmKARI2	Up	ZmKARI1	0.9349
			Ile	-0.8835
Metabolomics	Trp	Down	ZmKARI1	-0.9177
			ZmKARI2	-0.8847
	Ile	Down	*ZmBCAT4*	0.9263
			ZmKARI2	-0.8835
			Leu	0.9708
	Gln	Down	ZmAHAS1	0.9024
			Leu	-0.8897
	Gly	Down	ZmKARI1	0.8926
	Urea	Up	ZmAHAS1	0.9342
	Leu	Down	*ZmBCAT4*	0.9451
			Ile	0.9708
	Phe	Down	*ZmBCAT4*	0.9085
			Val	0.9188
	Pro	Down	*ZmBCAT4*	0.9371
			Val	0.9935
	Val	Down	*ZmBCAT4*	0.9584

[a]Transcripts or metabolites that showed significant changes in *ZmASR1* -OE leaves compared to WT leaves ($P < 0.05$, except transcripts in italic in which $P < 0.10$) .

[b]Transcripts or metabolites involved in the BCAA biosynthetic pathway and showing significant changes in *ZmASR1* -OE leaves compared to WT leaves ($P < 0.05$, except transcripts in italic in which $P < 0.10$) .

[c]Correlations were calculated from residual data. Green and red shading distinguish negative and positive correlations, respectively ($P < 0.05$). The original data are in the Supplemental Table S8A.

Table S11. Pair-wise correlations of ZmASR1 target transcripts against decreased and/or biomass-related metabolites

Parameter x[a]	Trend in *ZmASR1*-OE	Parameter y[b]	corr(x,y)[c]
ZmAHAS1	Up	Gln	0.9024
ZmBCAT4	Up	Ile	0.9263
		Leu	0.9451
		Phe	0.9085
		Pro	0.9371
		Val	0.9584
ZmKARI1	Up	Gly	0.8926
		Trp	-0.9177
ZmKARI2	Up	Ile	-0.8835
		Trp	-0.8847
ZmP5CS2	Up	Monomethylphosphate	-0.9352
		Raffinose	-0.9108
ZmP5CS3	Up	Ascorbate	-0.8937
		Citrate	-0.9840
		Galactinol	-0.8950
		Glc	-0.8904
		Malate	-0.9642
		Raffinose	-0.9067
		Suc	-0.9731
ZmSPL14	Up	Nicotinate	0.9884
MZ00000739		Spermidine	0.9159
ZmUSPA.1	Up	Benzoate	-0.9536
MZ00024643		Citrate	-0.9608
		Galactinol	-0.9509
		Malate	-0.8919
		Monomethylphosphate	-0.9021
		Raffinose	-0.9734
ZmWD40.1	Down	*trans*-Aconitate	-0.9961
MZ00022082		Ala	-0.9587
		Citramalate	-0.9738
		Glc	-0.9639
		Malate	-0.9195

[a]Transcripts that showed significant changes in *ZmASR1*-OE leaves compared to WT leaves ($P < 0.05$, except transcripts in italic in which $P < 0.10$) .

[b]Metabolites that showed significant decreases in *ZmASR1*-OE leaves compared to WT leaves ($P < 0.05$) and/or were correlated to biomass in Arabidopsis (Meyer et al., 2007; Sulpice et al., 2009). Green and red distinguish metabolites negatively and positively correlated to biomass, respectively, in Arabidopsis (Meyer et al., 2007; Sulpice et al., 2009).

[c]Correlations were calculated from residual data. Green and red shading distinguish negative and positive correlations, respectively ($P < 0.05$). The original data are in the Supplemental Table S8A.

Supplemental literature cited

Arcade A, Labourdette A, Falque M, Mangin B, Chardon F, Charcosset A, Joets J (2004) BioMercator: integrating genetic maps and QTL towards discovery of candidate genes. Bioinformatics **20:** 2324-2326

Romero P, Obradovic Z, Li X, Garner EC, Brown CJ, Dunker AK (2001) Sequence complexity of disordered protein. Proteins **42:** 38–48